Searches for the Chiral Magnetic Effect with ALICE

A. Dobrin for the ALICE Collaboration
(Institute of Space Science – INFLPR Subsidiary)

Chiral effects in heavy-ion collisions

G-R. Liang et al., CPC 44, 094103 (2020)

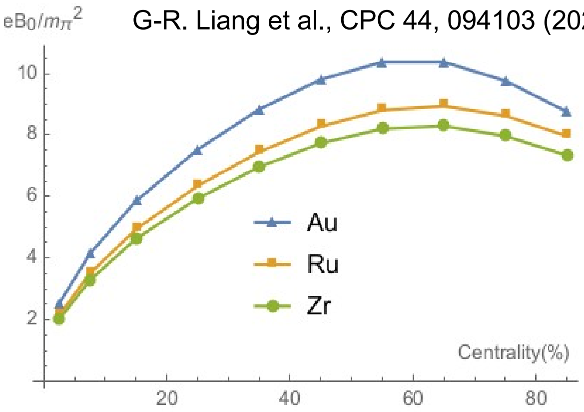

Heavy-ion collisions:
Strong magnetic field (B~10^{15} T)

http://www.physics.adelaide.edu.au/theory/staff/leinweber/VisualQCD/Nobel/

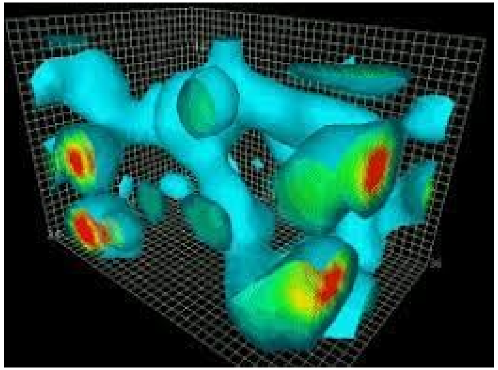

QCD domains with P and CP symmetries locally broken

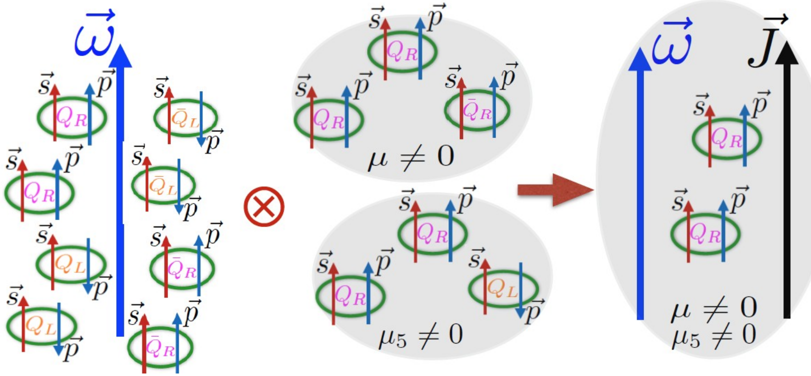

Electric current along the magnetic field → charge separation

Chiral Magnetic Effect (CME)

$$J_{\mathrm{V}}^{\mathrm{CME}} = \frac{\mu_{\mathrm{A}}}{2\pi^2} e\vec{B}$$

D. Kharzeev, PLB 633, 260 (2006); D. Kharzeev et al., NPA 797, 67 (2007); D. Son et al., PRL 103, 191601 (2009); Y. Burnier et al., PRL 107, 052303 (2011); D. Kharzeev, PRL 106, 062301 (2011); D. Kharzeev et al., PRD 83, 085007 (2011); D. Kharzeev et al, PPNP 88, 1 (2016)

Chiral effects in heavy-ion collisions

G-R. Liang et al., CPC 44, 094103 (2020)

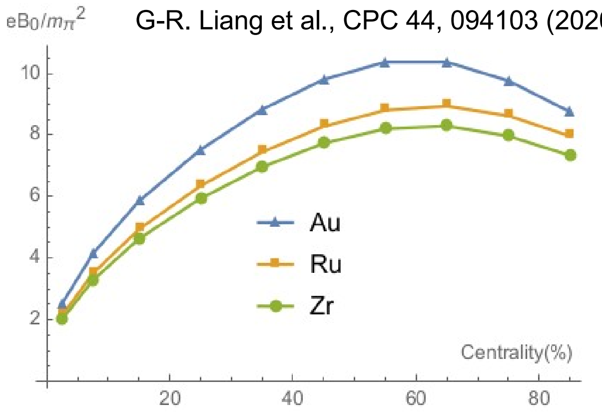

Heavy-ion collisions:
Strong magnetic field (B~10^{15} T)

http://www.physics.adelaide.edu.au/theory/staff/leinweber/VisualQCD/Nobel/

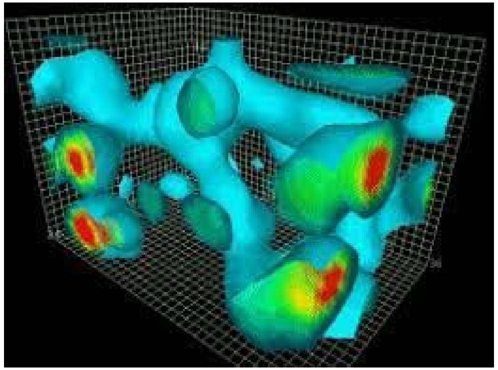

QCD domains with P and CP symmetries locally broken

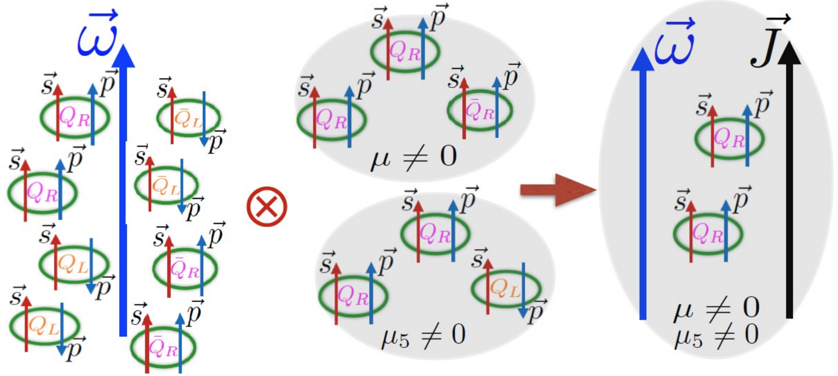

Electric current along the magnetic field → charge separation

Chiral Magnetic Effect (CME)

$$J_{\mathrm{V}}^{\mathrm{CME}} = \frac{\mu_{\mathrm{A}}}{2\pi^2} e\vec{B}$$

D. Kharzeev, PLB 633, 260 (2006); D. Kharzeev et al., NPA 797, 67 (2007); D. Son et al., PRL 103, 191601 (2009); Y. Burnier et al., PRL 107, 052303 (2011); D. Kharzeev, PRL 106, 062301 (2011); D. Kharzeev et al., PRD 83, 085007 (2011); D. Kharzeev et al, PPNP 88, 1 (2016)

Interpretation of the results complicated by background contributions

Observables

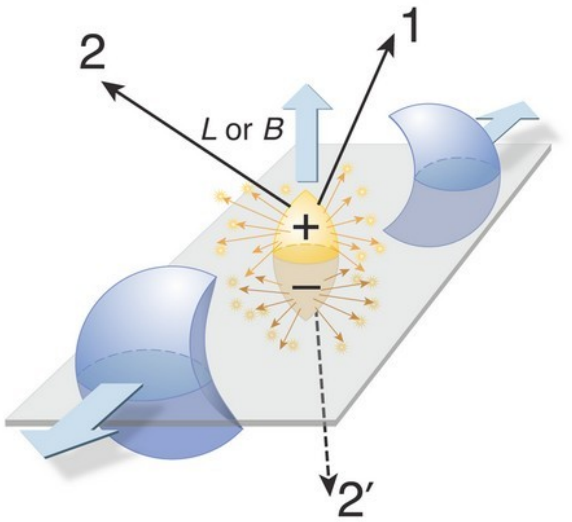

$$\frac{dN}{d\Delta\varphi_\alpha} \sim 1 + 2v_{1,\alpha}\cos(\Delta\varphi_\alpha) + 2a_{1,\alpha}\sin(\Delta\varphi_\alpha) + 2v_{2,\alpha}\cos(2\Delta\varphi_\alpha) + \ldots,$$

2-particle correlator

$$\delta_m = \langle \cos[m(\varphi_a - \varphi_b)] \rangle$$

STAR, PRC 81, 054908 (2009)

$$\langle \cos(\varphi_a - \varphi_b) \rangle = \langle \cos[(\varphi_a - \Psi_{RP}) - (\varphi_b - \Psi_{RP})] \rangle$$
$$= \langle \cos(\Delta\varphi_a - \Delta\varphi_b) \rangle = \langle v_{1,a} v_{1,b} \rangle + \langle a_{1,a} a_{1,b} \rangle + B_{in} + B_{out}$$

Observables

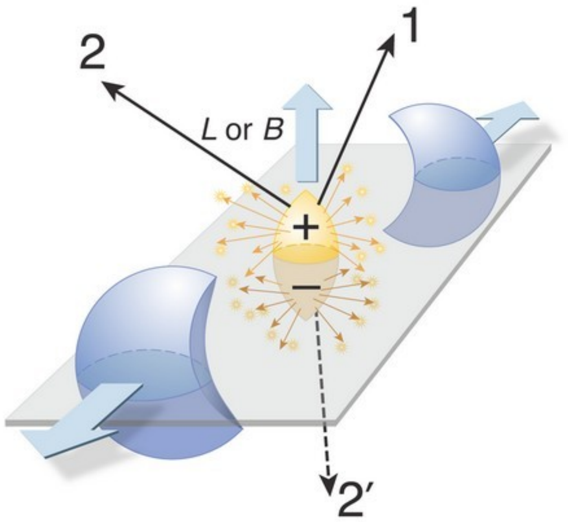

$$\frac{dN}{d\Delta\varphi_\alpha} \sim 1 + 2v_{1,\alpha}\cos(\Delta\varphi_\alpha) + 2a_{1,\alpha}\sin(\Delta\varphi_\alpha) + 2v_{2,\alpha}\cos(2\Delta\varphi_\alpha) + ...,$$

2-particle correlator

STAR, PRC 81, 054908 (2009)

$$\delta_m = \langle \cos[m(\varphi_a - \varphi_b)]\rangle$$

$$\langle \cos(\varphi_a - \varphi_b)\rangle = \langle \cos[(\varphi_a - \Psi_{\mathrm{RP}}) - (\varphi_b - \Psi_{\mathrm{RP}})]\rangle$$
$$= \langle \cos(\Delta\varphi_a - \Delta\varphi_b)\rangle = \langle v_{1,a} v_{1,b}\rangle + \langle a_{1,a} a_{1,b}\rangle + B_{\mathrm{in}} + B_{\mathrm{out}}$$

3-particle correlator

S. Voloshin, PRC 70, 057901 (2004)

$$\gamma_{m,n} = \langle \cos(m\varphi_a + n\varphi_b - (m+n)\Psi_{|m+n|})\rangle$$

$$\langle \cos(\varphi_a + \varphi_b - 2\Psi_{\mathrm{RP}})\rangle = \langle \cos[(\varphi_a - \Psi_{\mathrm{RP}}) + (\varphi_b - \Psi_{\mathrm{RP}})]\rangle$$
$$= \langle \cos(\Delta\varphi_a - \Delta\varphi_b)\rangle = \langle v_{1,a} v_{1,b}\rangle - \langle a_{1,a} a_{1,b}\rangle + B_{\mathrm{in}} - B_{\mathrm{out}}$$

Observables

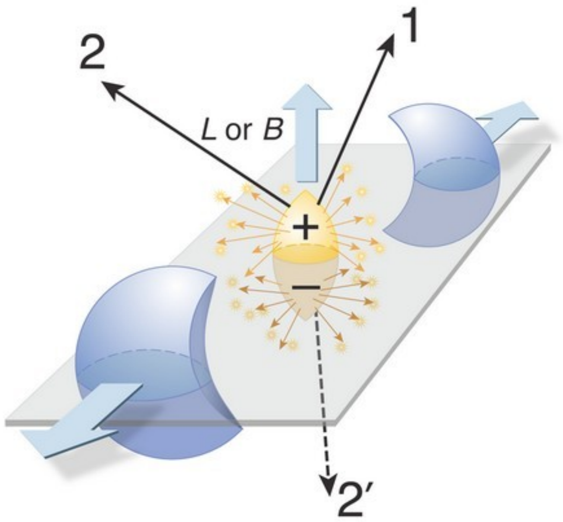

$$\frac{dN}{d\Delta\varphi_\alpha} \sim 1 + 2v_{1,\alpha}\cos(\Delta\varphi_\alpha) + 2a_{1,\alpha}\sin(\Delta\varphi_\alpha) + 2v_{2,\alpha}\cos(2\Delta\varphi_\alpha) + \ldots,$$

2-particle correlator

STAR, PRC 81, 054908 (2009)

$$\delta_m = \langle \cos[m(\varphi_a - \varphi_b)] \rangle$$

$$\langle \cos(\varphi_a - \varphi_b) \rangle = \langle \cos[(\varphi_a - \Psi_{RP}) - (\varphi_b - \Psi_{RP})] \rangle$$
$$= \langle \cos(\Delta\varphi_a - \Delta\varphi_b) \rangle = \langle v_{1,a} v_{1,b} \rangle + \langle a_{1,a} a_{1,b} \rangle + B_{in} + B_{out}$$

3-particle correlator

S. Voloshin, PRC 70, 057901 (2004)

$$\gamma_{m,n} = \langle \cos(m\varphi_a + n\varphi_b - (m+n)\Psi_{|m+n|}) \rangle$$

$$\langle \cos(\varphi_a + \varphi_b - 2\Psi_{RP}) \rangle = \langle \cos[(\varphi_a - \Psi_{RP}) + (\varphi_b - \Psi_{RP})] \rangle$$
$$= \langle \cos(\Delta\varphi_a - \Delta\varphi_b) \rangle = \langle v_{1,a} v_{1,b} \rangle - \langle a_{1,a} a_{1,b} \rangle + B_{in} - B_{out}$$

“Flowing clusters”

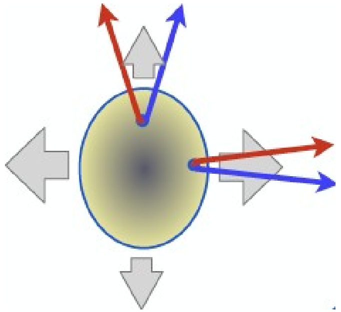

B_{in} and B_{out} background contributions projected onto Ψ_{RP} and perpendicular to it

$$B_{in} - B_{out} \propto v_{2,\mathrm{cluster}} \langle \cos(\varphi_a + \varphi_b - 2\varphi_{\mathrm{cluster}}) \rangle$$

Anisotropic flow

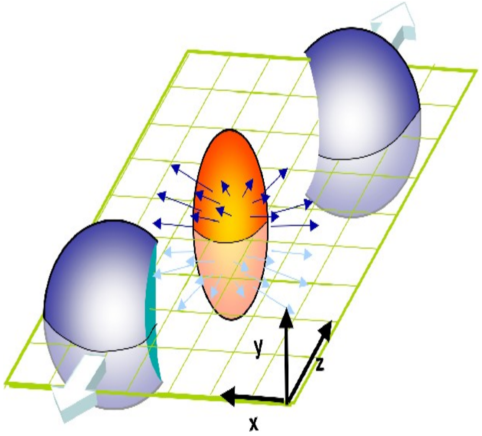

Anisotropic flow

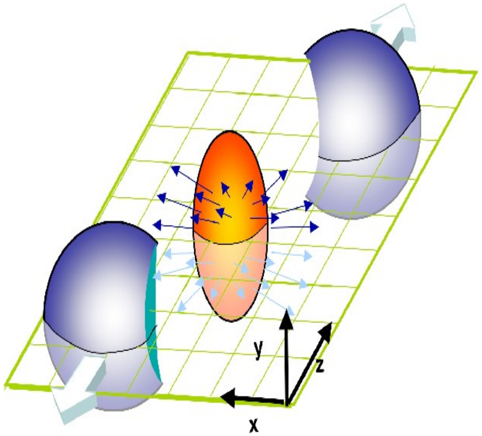

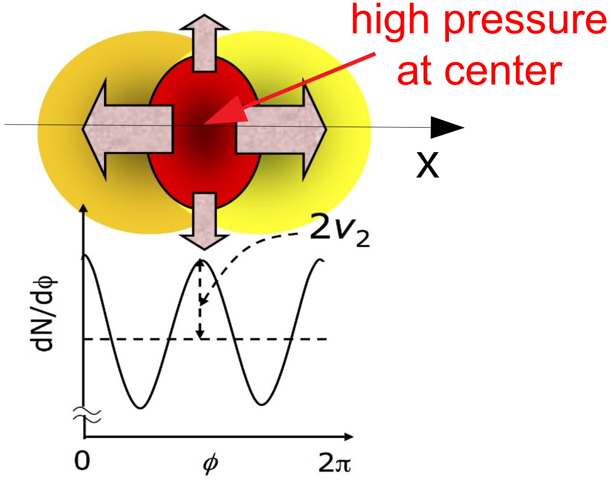

Pressure gradients (larger in the x direction) push bulk “out” → “flow”

More particles seen in the x-direction

Anisotropic flow

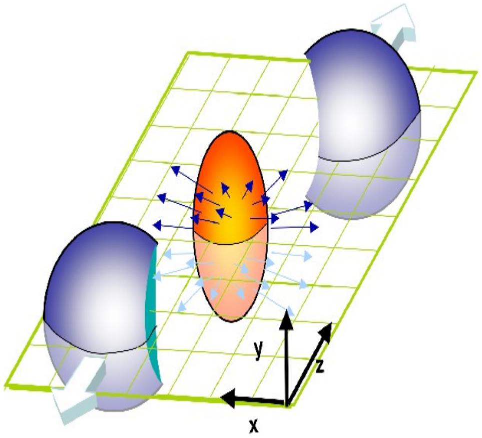

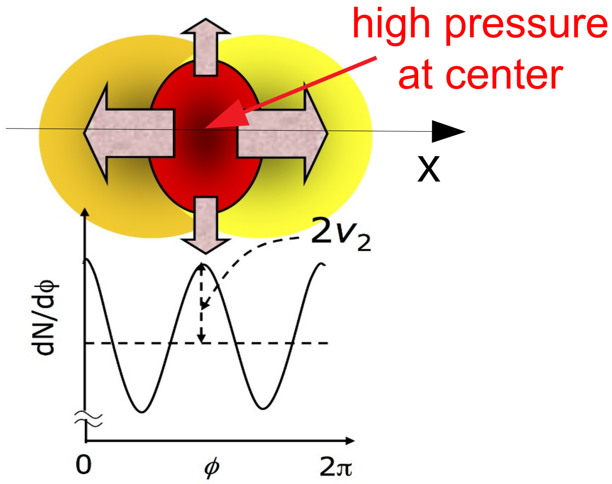

Pressure gradients (larger in the x direction) push bulk “out” → “flow”

More particles seen in the x-direction

$$E\frac{d^3N}{d^3p}=\frac{1}{2\pi}\frac{d^2N}{p_T\,dp_T\,dy}\left(1+\sum_{n=1}^{\infty}2v_n\cos\left(n\left(\varphi-\Psi_n\right)\right)\right)$$

- Anisotropic flow: initial spatial anisotropy → final momentum anisotropy via collective interactions

Anisotropic flow

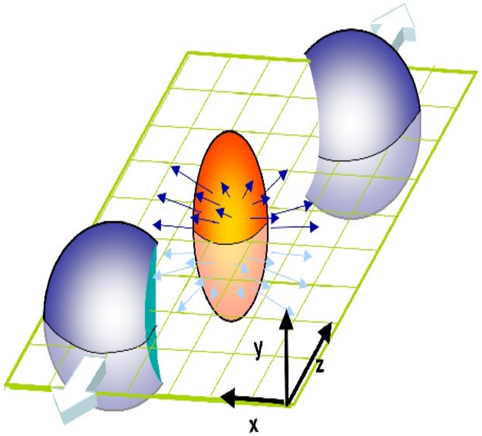

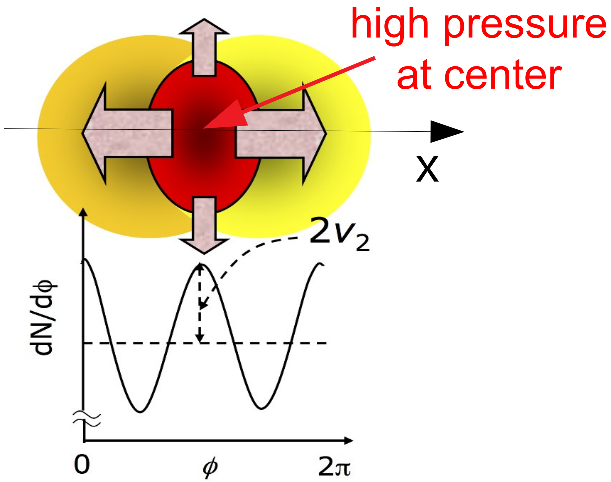

Pressure gradients (larger in the x direction) push bulk "out" → "flow"

More particles seen in the x-direction

ALICE, arXiv:2211.04384

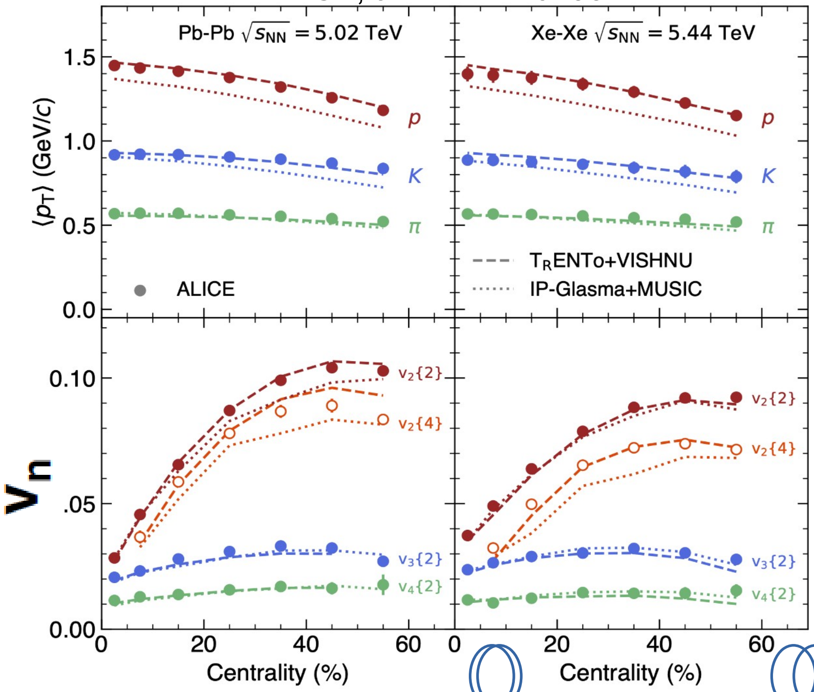

$$E\frac{d^3N}{d^3p}=\frac{1}{2\pi}\frac{d^2N}{p_T\,dp_T\,dy}\left(1+\sum_{n=1}^{\infty}2v_n\cos\left(n\left(\varphi-\Psi_n\right)\right)\right)$$

- Anisotropic flow: initial spatial anisotropy → final momentum anisotropy via collective interactions
  - v_n quantify the event anisotropy

Anisotropic flow

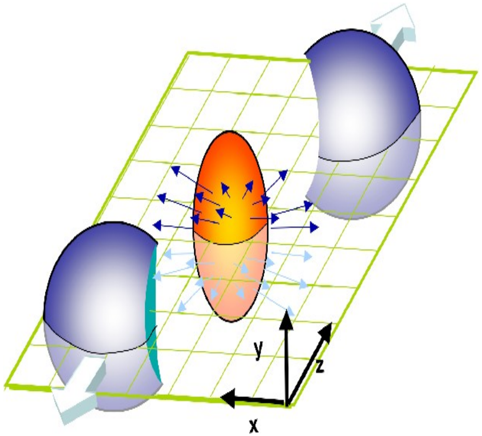

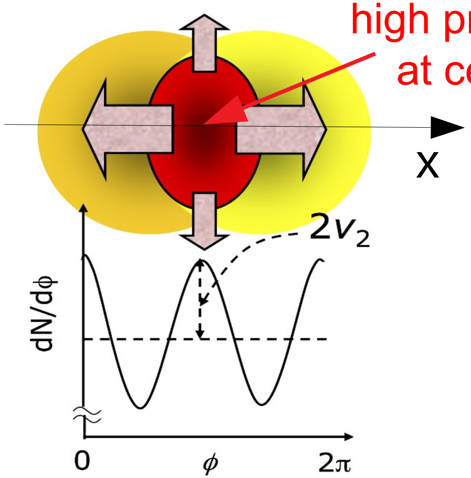

Pressure gradients (larger in the x direction) push bulk "out" → "flow"

More particles seen in the x-direction

J. Bernhard et al., NP 19 (2019) 1113

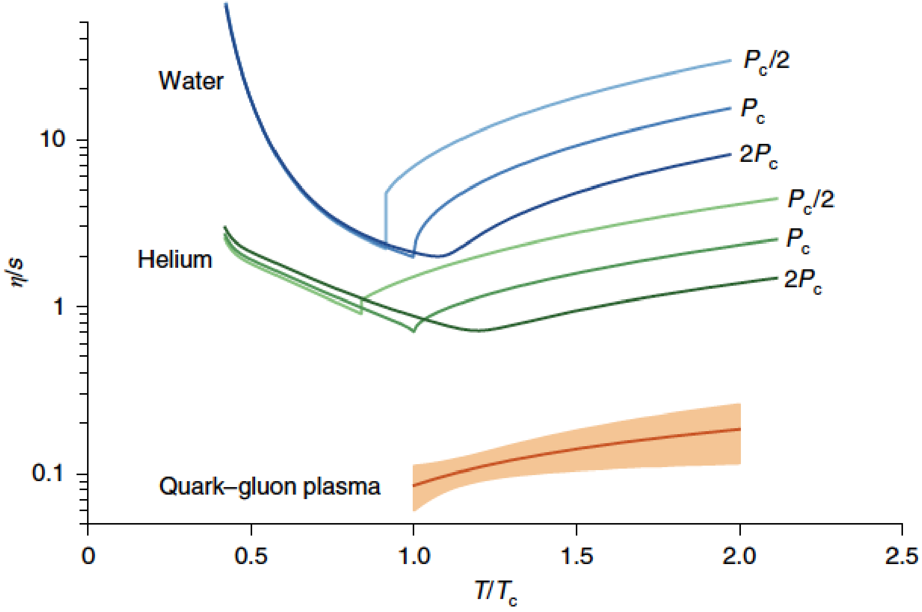

$$E\frac{d^3N}{d^3p}=\frac{1}{2\pi}\frac{d^2N}{p_T\,dp_T\,dy}\left(1+\sum_{n=1}^{\infty}2v_n\cos\left(n\left(\varphi-\Psi_n\right)\right)\right)$$

- Anisotropic flow: initial spatial anisotropy → final momentum anisotropy via collective interactions
  - v_n quantify the event anisotropy
- Characterize key QGP properties like viscosity
  - Nearly perfect fluid: $1/4\pi < \eta/s < 3/4\pi$

A Large Ion Collider Experiment

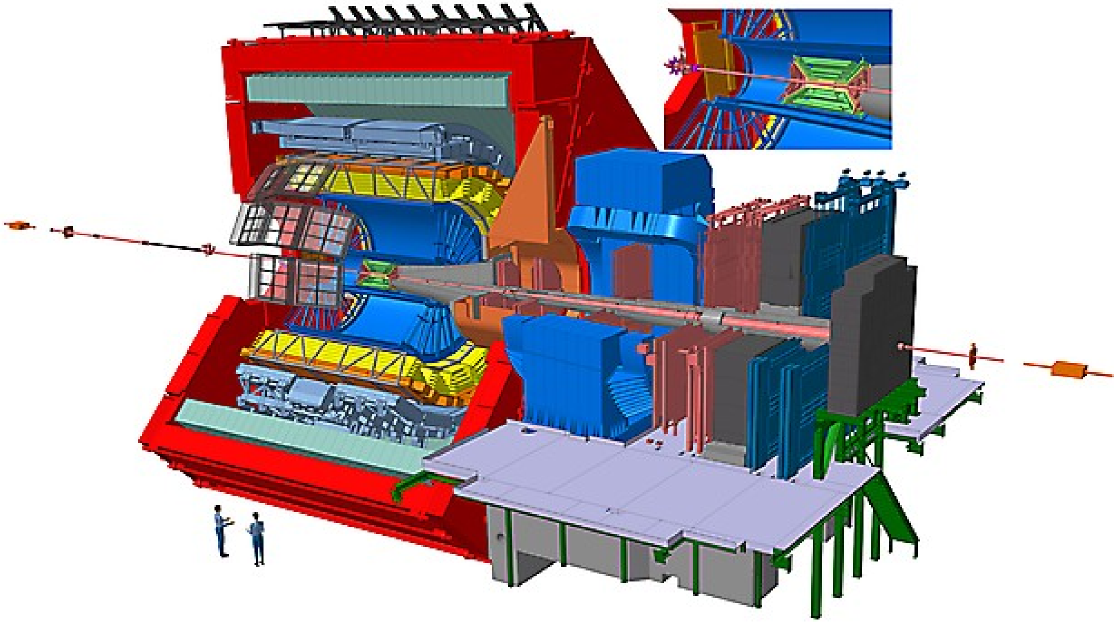

- Inner Tracking System (ITS)
  - Tracking, vertexing
- Time Projection Chamber (TPC)
  - Tracking, vertexing, particle identification based on specific energy loss, Ψ_n
- Time-of-Flight (TOF)
  - Particle identification based on flight time
- V0 detector
  - Triggering, centrality, Ψ_n

- Track selection
  - $0.2 < p_T < 5$ GeV/c, $|\eta| < 0.8$

q_2 selection	v_n/CME/Ψ_n	Ψ_n
V0C	TPC	V0A
$-3.7<\eta<-1.7$	$-0.8<\eta<0.8$	$2.8<\eta<5.1$

η

- Pb–Pb at $\sqrt{s_{NN}}$ = 5.02 TeV
  - ~235M events
- Xe–Xe at $\sqrt{s_{NN}}$ = 5.44 TeV
  - ~1M events

CME @ LHC

ALICE, EPJC 84, 813 (2024)

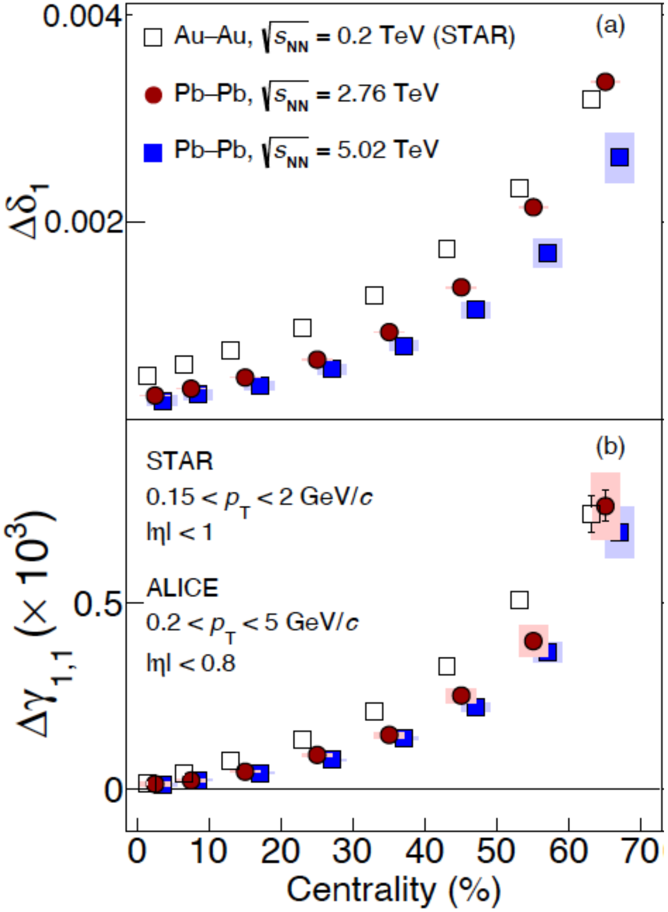

- Strong centrality dependence consistent with naive expectations from CME
- Similar magnitude between RHIC and LHC
  - Different dilution effects (3x larger dN_{ch}/dη at LHC than at RHIC)
  - Different magnitude of the magnetic field
- Large contribution from background → local charge conservation (LCC) coupled with anisotropic flow

S. Schlichting and S. Pratt, PRC 83, 014913 (2011)

  - Various approaches used to disentangle signal from background
    - Vary the background (v_2) → event shape engineering
    - “Killing” the signal (B) → higher harmonics
    - Vary the signal (B) → different collision systems

CME @ LHC

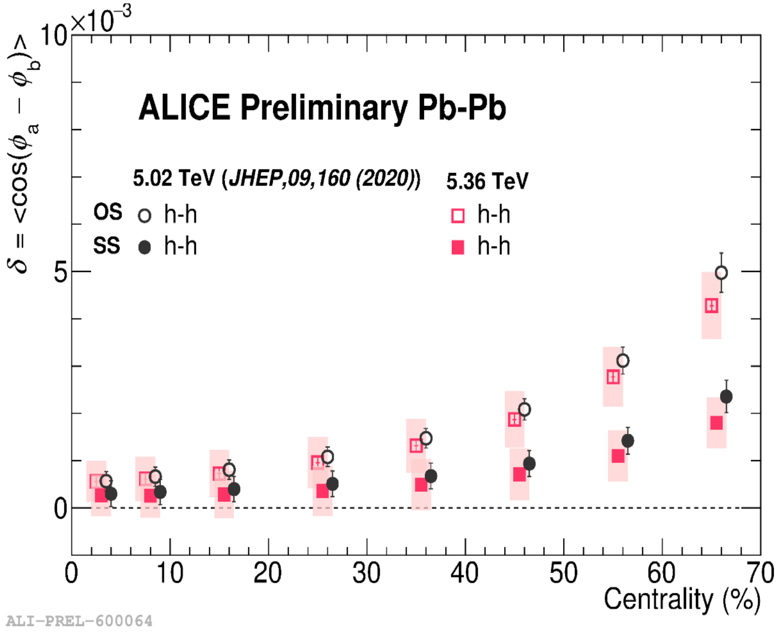

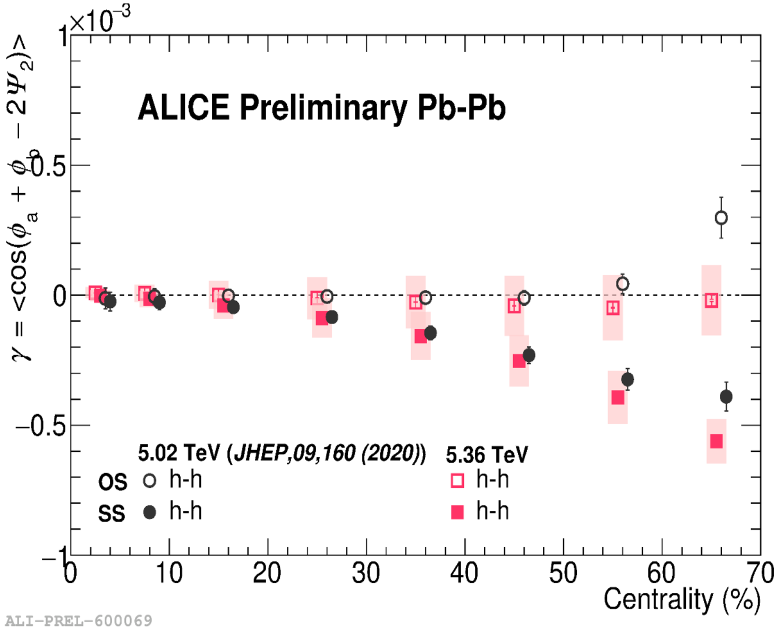

- (Almost) no dependence on collision energy
  - Non-flow contributions affect measurements in peripheral collisions

Varying the background using event shape engineering

Event Shape Engineering (ESE)

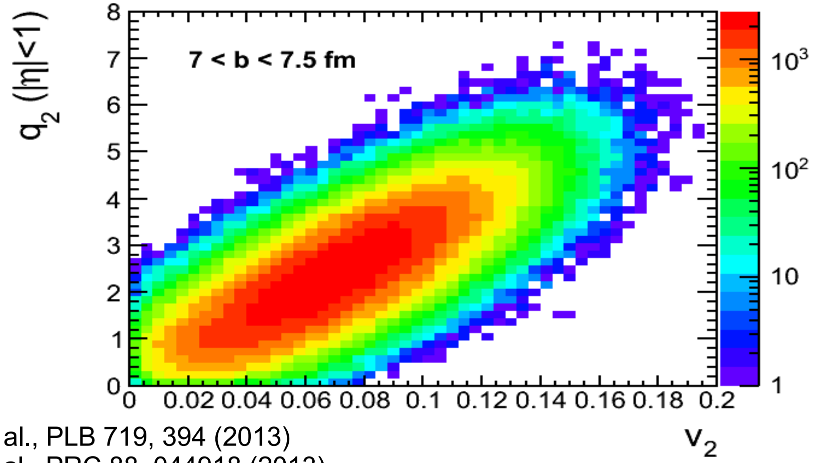

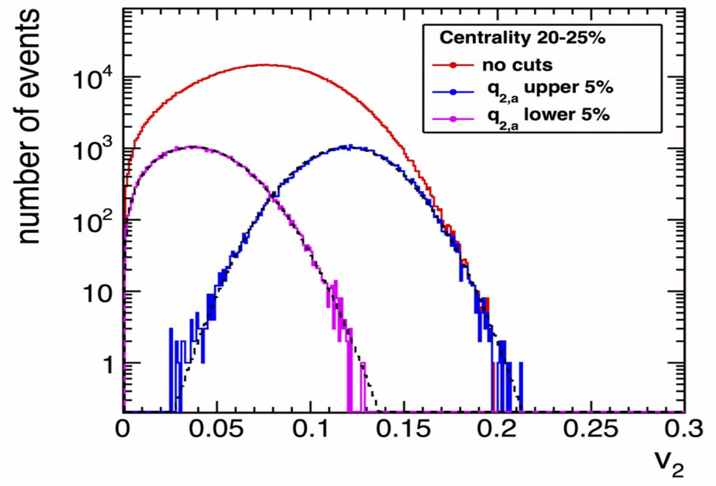

J. Schukraft et al., PLB 719, 394 (2013)
H. Petersen et al., PRC 88, 044918 (2013)
P. Huo et al., PRC 90, 024910 (2014)

- Select events with similar centralities and different shapes based on the event-by-event flow/eccentricity fluctuations

Flow vector

$$Q_{n,x} = \sum_i \cos(n\varphi_i)$$
$$Q_{n,y} = \sum_i \sin(n\varphi_i)$$

q_n distribution

$$Q_n = Q_{n,x}, iQ_{n,y}$$
$$q_n = |Q_n| / \sqrt{M}$$

CME with ESE (I)

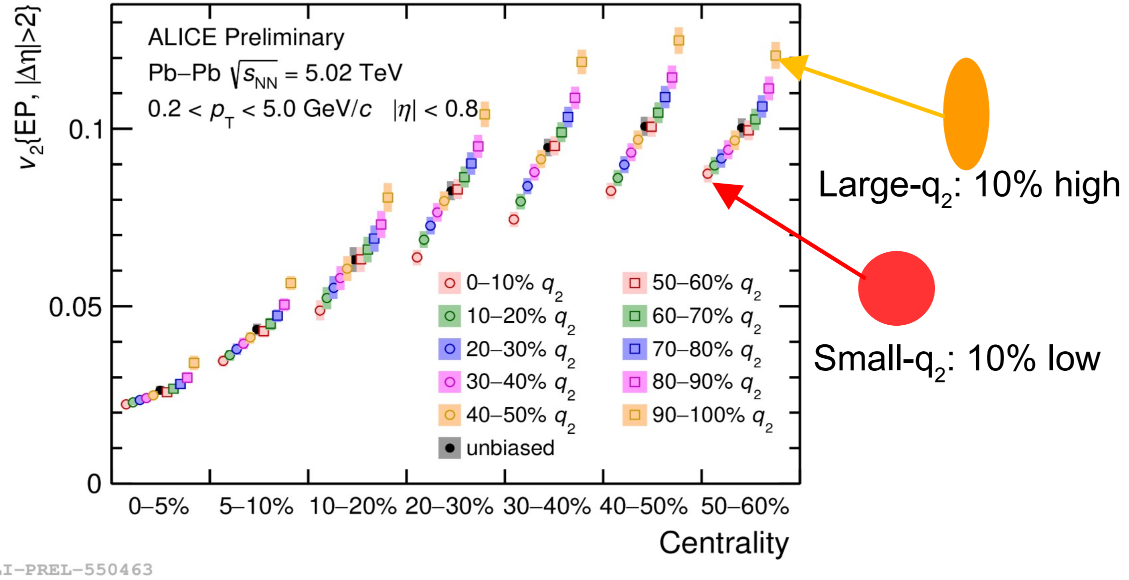

- q_2^{V0C} used to select events with 30% larger or 25% smaller v_2 than the average

CME with ESE (I)

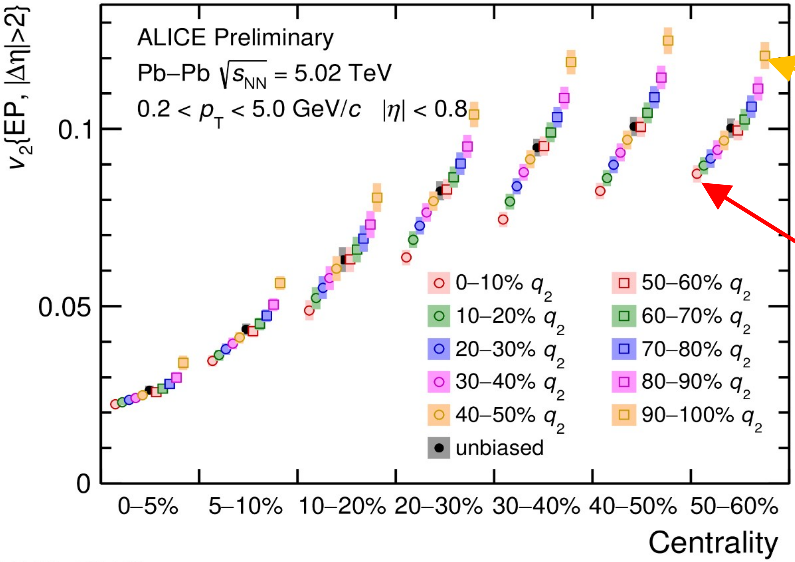

ALI-PREL-550463

Large-q_2: 10% high

Small-q_2: 10% low

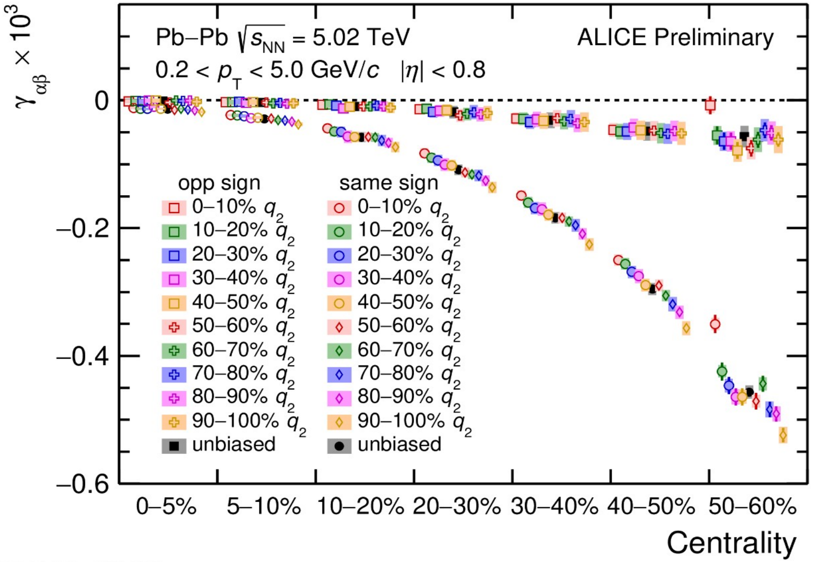

ALI-PREL-550472

- q_2^{V0C} used to select events with 30% larger or 25% smaller v_2 than the average
- $\gamma_{\alpha\beta}$ contains potential CME signal as well as background effects
  - Background contributions are suppressed at the level of v_2
- $\gamma_{\alpha\beta}$ depends on the event shape selection in a given centrality bin

CME with ESE (II)

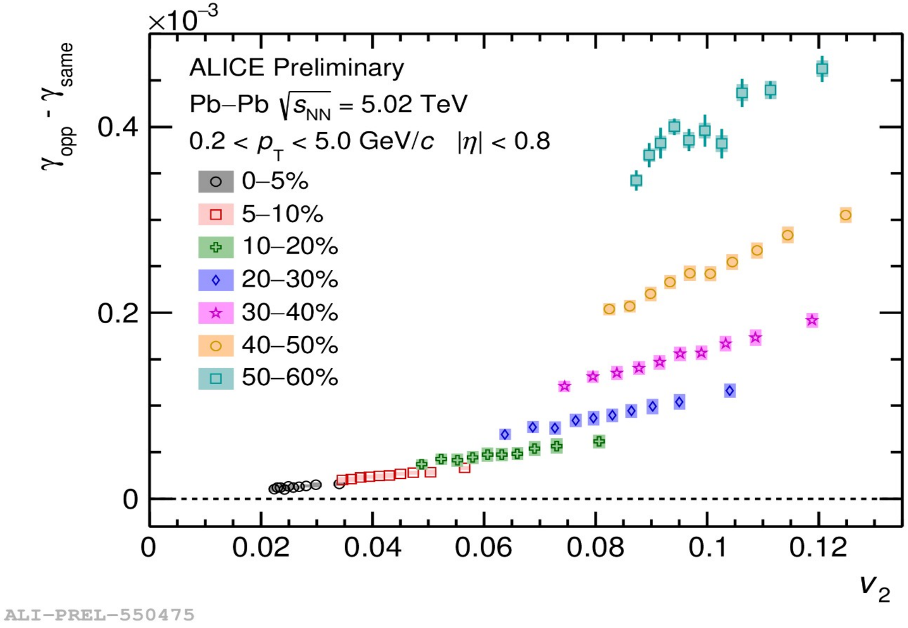

- γ_{ab} (opp-same) can be used to study the CME
  - Difference is positive for all centrality classes and decreases with centrality and v_2 (in a given centrality bin)

CME with ESE (II)

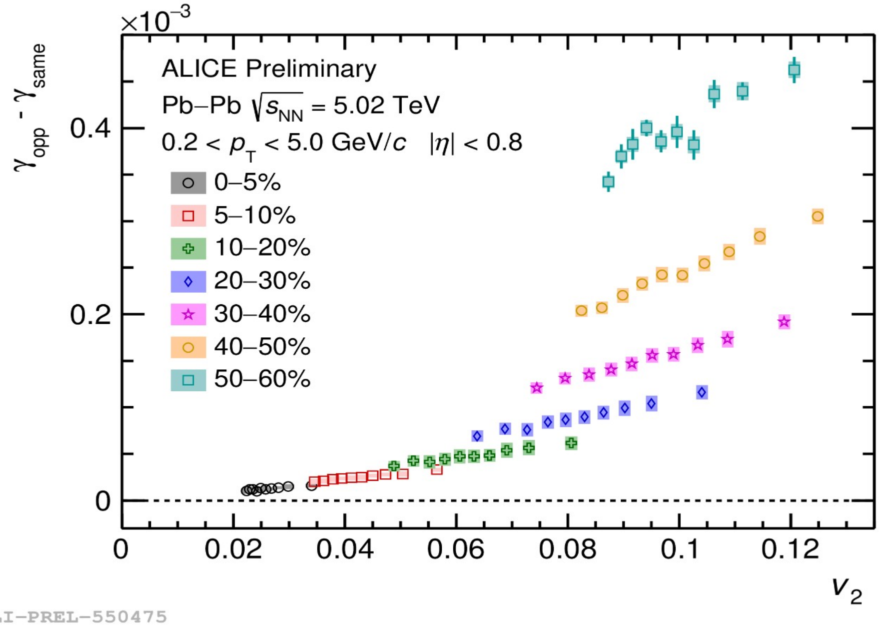

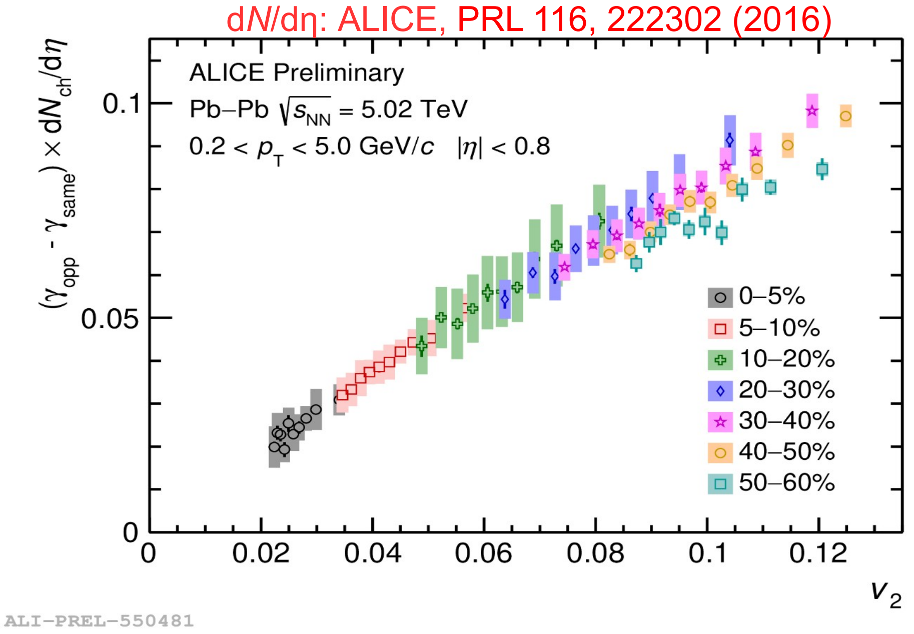

- γ_{ab} (opp-same) can be used to study the CME
  - Difference is positive for all centrality classes and decreases with centrality and v_2 (in a given centrality bin)
  - Difference approximately scales with v_2 and multiplicity → mostly background contribution

Does magnetic field depend on v_2 in initial state models?

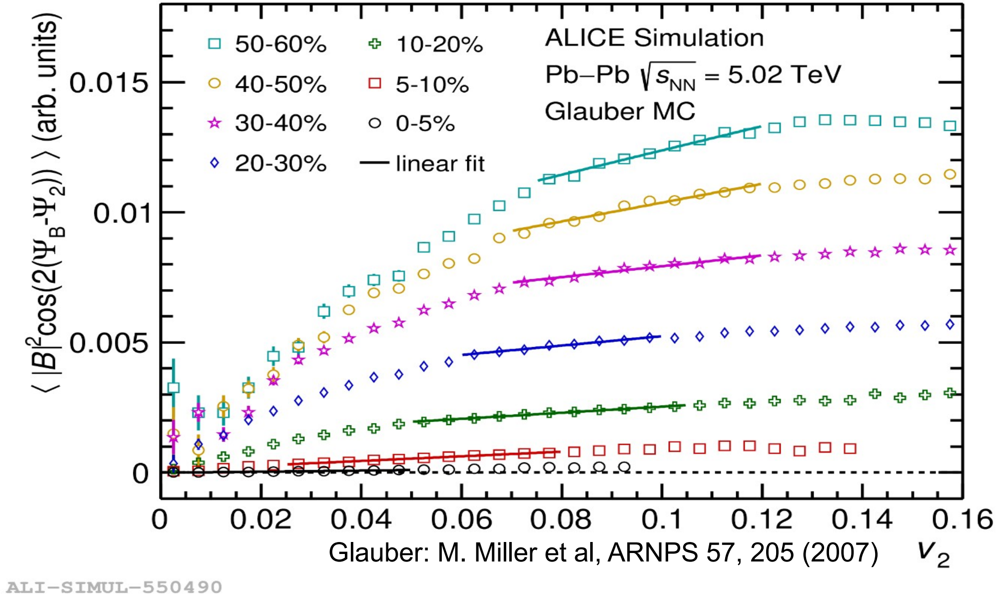

Glauber: M. Miller et al, ARNPS 57, 205 (2007)

$$eB_s^{\pm}(\tau,\eta,\boldsymbol{x}_\perp) = \pm Z\alpha_{EM}\sinh(Y_0 \mp \eta)\int \mathrm{d}^2\boldsymbol{x}'_\perp \rho_\pm(\boldsymbol{x}'_\perp)[1-\theta_\mp(\boldsymbol{x}'_\perp)] \times \frac{(\boldsymbol{x}'_\perp - \boldsymbol{x}_\perp)\times \boldsymbol{e}_z}{[(\boldsymbol{x}'_\perp - \boldsymbol{x}_\perp)^2 + \tau^2\sinh(Y_0 \mp \eta)^2]^{3/2}}$$

D. Kharzeev et al., NPA 803, 227 (2008)

- Perform a MC Glauber simulation to evaluate the dependence of the CME signal on v_2
  - Parameters are tuned to ALICE results
  - Calculate magnetic field at the origin using spectators with the proper time τ=0.1 fm
  - $\langle |B|^2\cos(2(\Psi_B-\Psi_2))\rangle$, the expected contribution of the CME to γ_{ab}, shows a strong dependence on v_2

Relating data and models

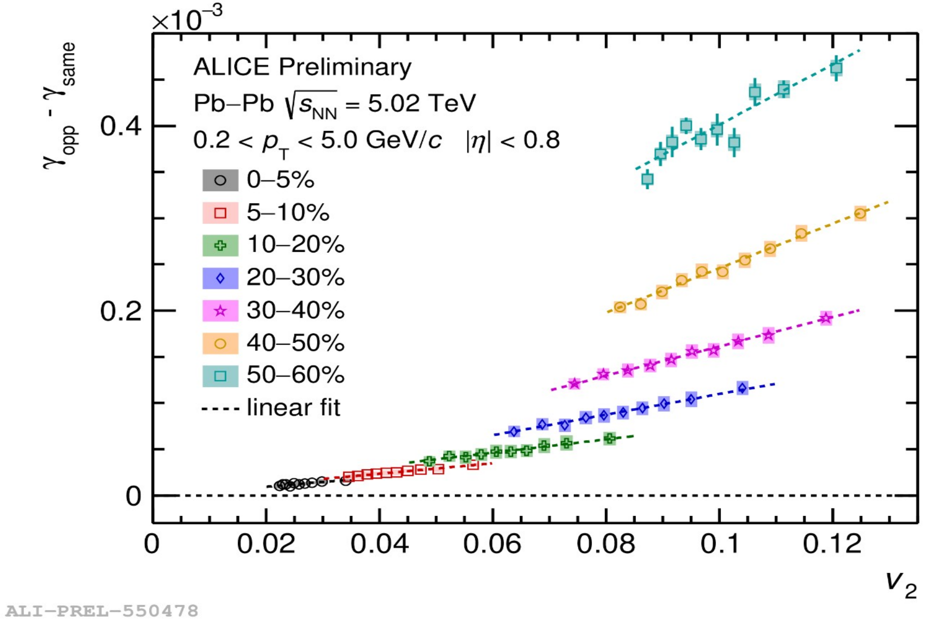

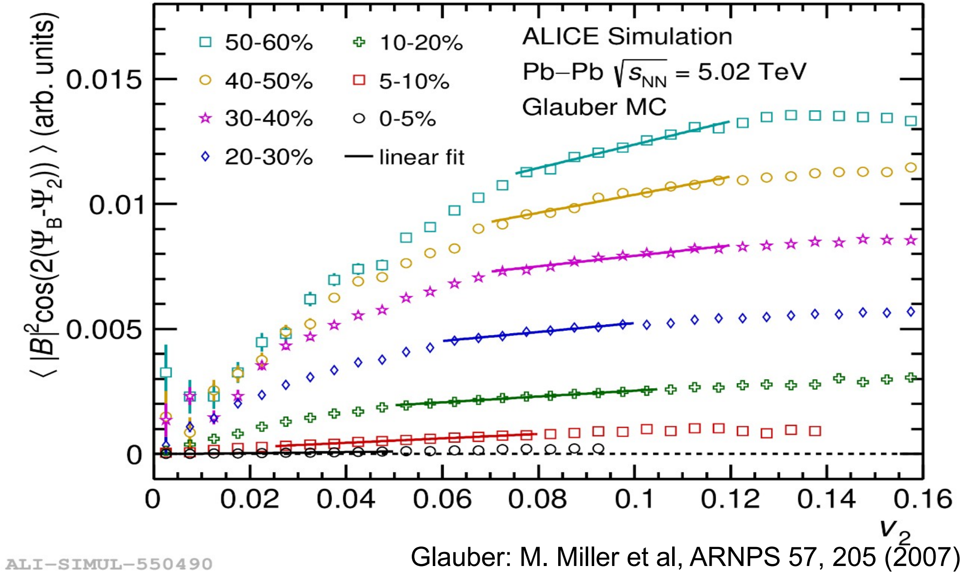

Glauber: M. Miller et al, ARNPS 57, 205 (2007)

- Fit γ_{ab} (opp-same) and $\langle |B|^2\cos(2(\Psi_B-\Psi_2))\rangle$ with a linear function to disentangle the potential CME signal from background

$$P_1(v_2) = p_0(1 + p_1(v_2 - \langle v_2 \rangle)/\langle v_2 \rangle)$$

Slopes of data and model fits

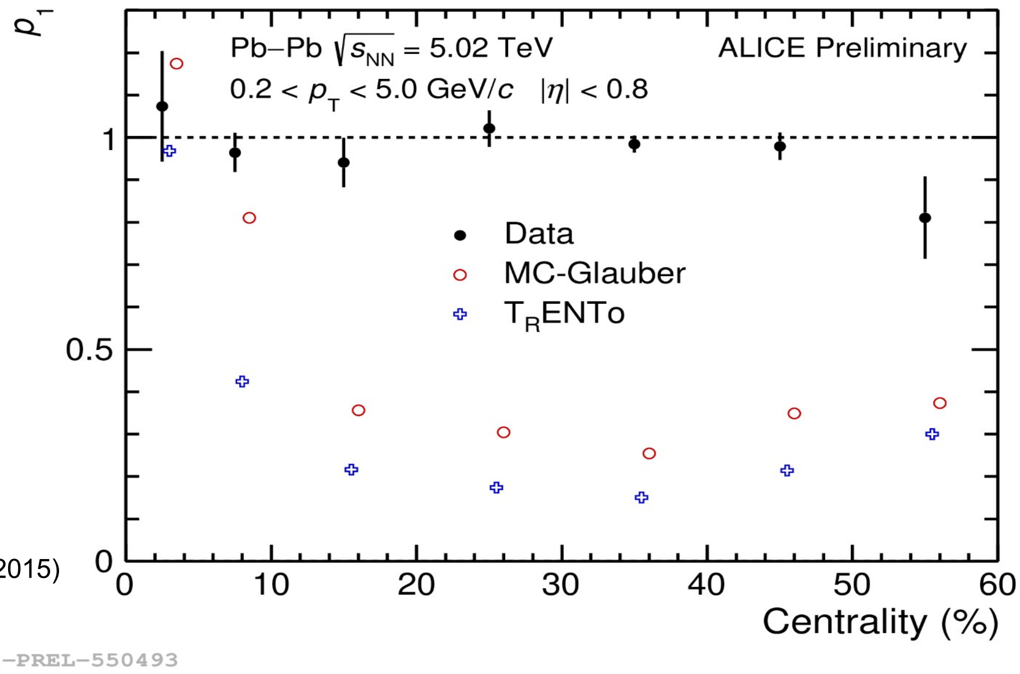

Glauber: M. Miller et al, ARNPS 57, 205 (2007)
TRENTO: J. Moreland et al, PRC 92, 011901 (2015)

- Extract the CME fraction, f_{CME} relating the slopes of data and model fits according to

$$f_{\mathrm{CME}} * p_{1,MC} + (1 - f_{\mathrm{CME}}) * 1 = p_{1,data}$$

- Assumption: background contribution scales linearly with v_2 and the corresponding slope is unity

CME fraction

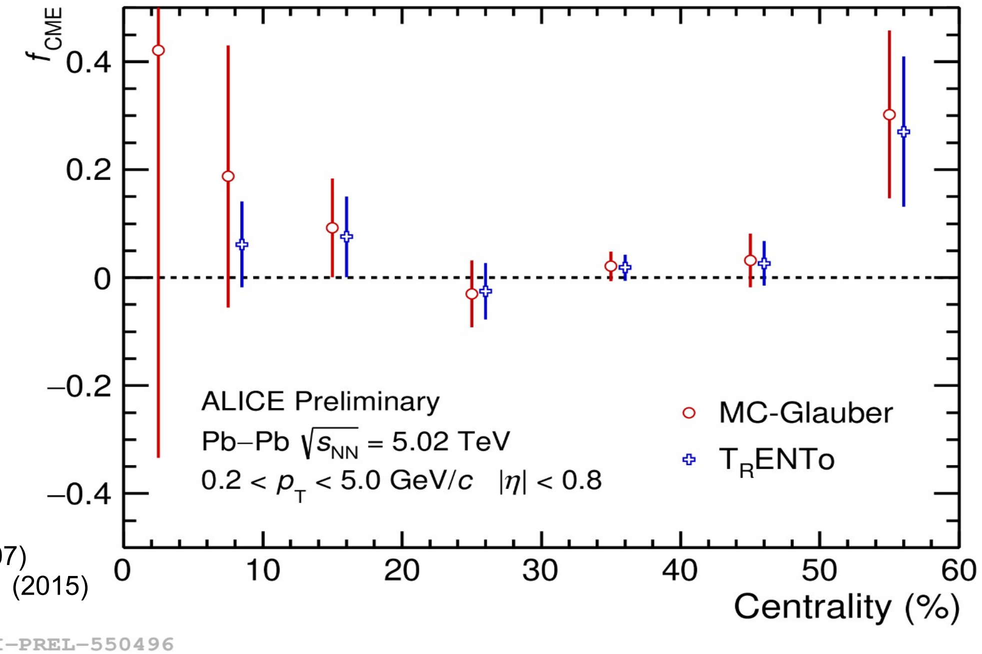

Glauber: M. Miller et al, ARNPS 57, 205 (2007)
TRENTO: J. Moreland et al, PRC 92, 011901 (2015)

- CME fraction in 0–5% is currently statistically limited
- Combining the points from 5–60% gives
  - f_{CME} (Glauber) = 0.028 ± 0.021 → 7% at 95% C.L.
  - f_{CME} (T$_R$ENTo) = 0.025 ± 0.018 → 6% at 95% C.L.

“Killing” the signal using higher harmonics

ALICE, JHEP 09, 160 (2020)

2-particle correlators

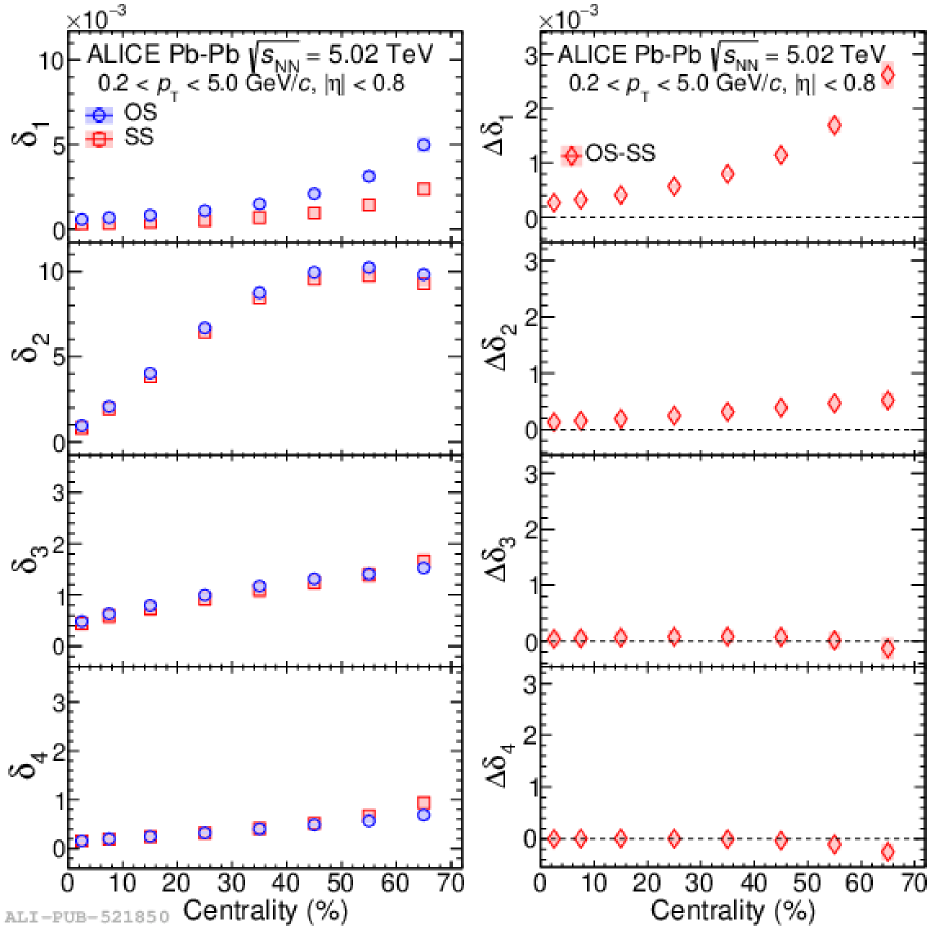

- Weak charge dependence, except δ_1
  - Dominated by background effects → constrain background in $\gamma_{1,1}$

3-particle correlators

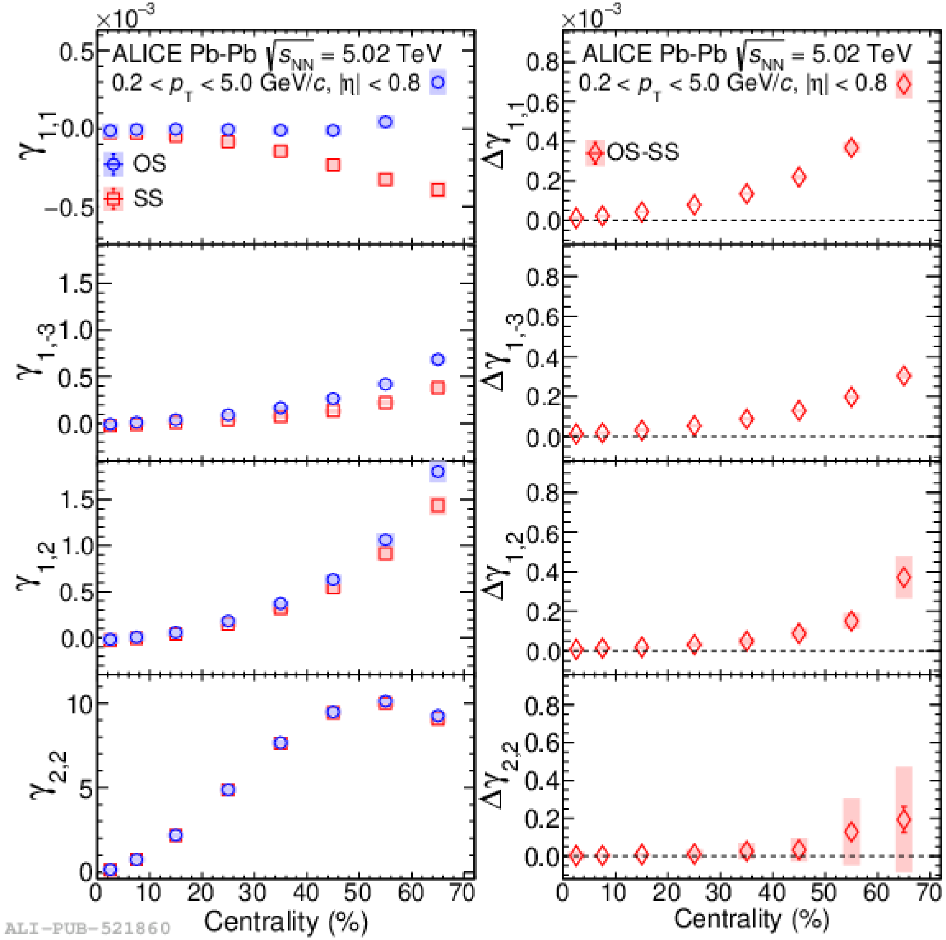

- $\gamma_{1,1}$ and $\gamma_{1,-3}$ sensitive to CME
- $\gamma_{1,2}$ and $\gamma_{2,2}$ probe only the background
- Significant charge dependence, except $\gamma_{2,2}$
  - Increases from central to peripheral collisions

3-particle correlators

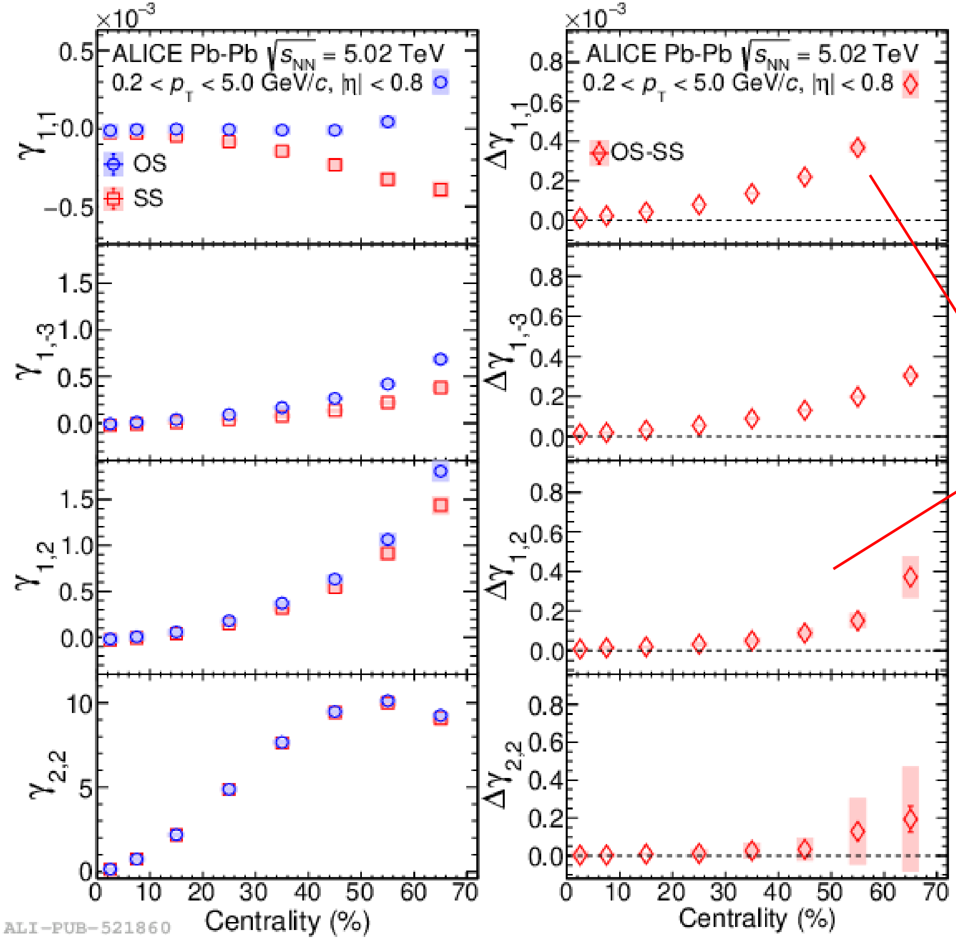

- $\gamma_{1,1}$ and $\gamma_{1,-3}$ sensitive to CME
- $\gamma_{1,2}$ and $\gamma_{2,2}$ probe only the background
- Significant charge dependence, except $\gamma_{2,2}$
  - Increases from central to peripheral collisions
- $\gamma_{1,1}$ and $\gamma_{1,2}$ used to estimate the background contribution to $\gamma_{1,1}$

$$\Delta\gamma_{1,1} \approx \kappa_2 v_2 \Delta\delta_1$$
$$\Delta\gamma_{1,2} \approx \kappa_3 v_3 \Delta\delta_1 \longrightarrow \Delta\gamma_{1,1}^{\rm Bkg} \approx \Delta\gamma_{1,2} \times \frac{v_2}{v_3}\frac{\kappa_2}{\kappa_3}$$
$$\Delta\gamma_{2,2} \approx \kappa_4 v_4 \Delta\delta_2$$

CME fraction

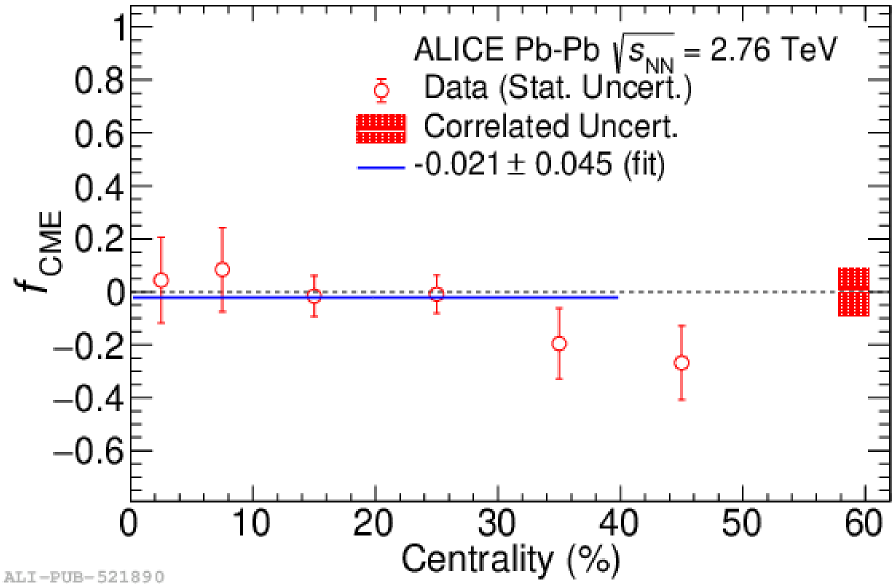

ALI-PUB-521890

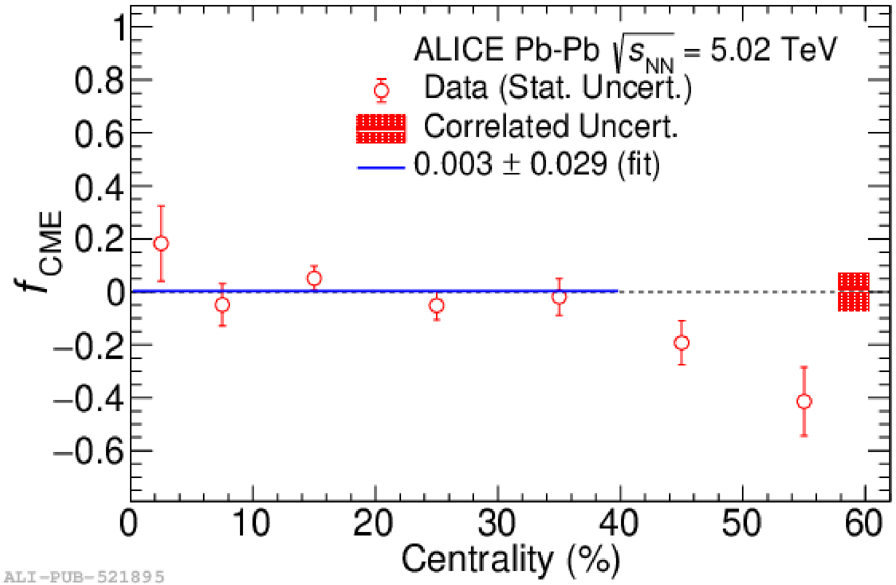

ALI-PUB-521895

- Consistent with 0 for 0–40% and then becomes negative
- Combining the points from 0–40%
  - $f_{CME}^{2.76\ \mathrm{TeV}}$ = -0.021 ± 0.045 → 18% at 95% C.L.
  - $f_{CME}^{5.02\ \mathrm{TeV}}$ = 0.003 ± 0.029 → 15% at 95% C.L.

$$f_{\mathrm{CME}} = 1 - \frac{\Delta\gamma_{1,1}^{\mathrm{Bkg}}}{\Delta\gamma_{1,1}}$$

Assumption: $\kappa_2 \approx \kappa_3$

Model comparisons

ALICE, arXiv: 2211.04384

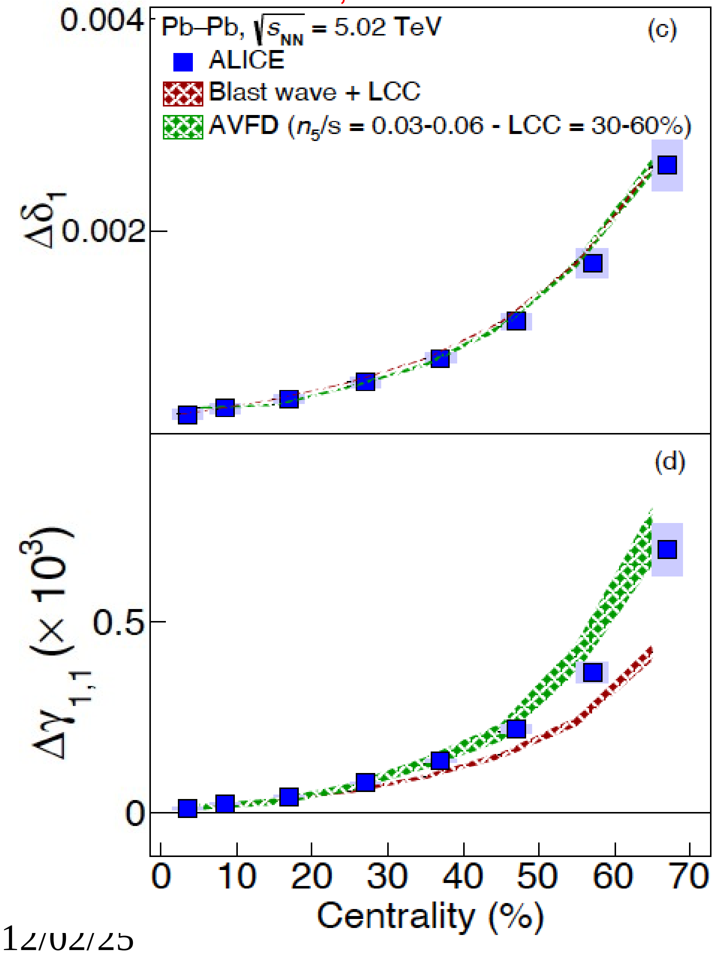

- Blast-Wave + Local Charge Conservation (LCC)
  - Tune the parameters in each centrality class to reproduce v_2 and p_T spectra of π, K, p
  - Tune the number of sources emitting balancing pairs
  - Underestimates $\Delta\gamma_{1,1}$ by up to ≈40%
    - Disagreement increases from central to peripheral collisions

- Anomalous Viscous Fluid Dynamics (AVFD)
  - EbyE IC + E/M fields (field lifetime as input)
  - Tune the parameters in each centrality class to reproduce v_2 and multiplicity
  - Good agreement with data points
    - Non-zero values for signal

P. Christakoglou et al., EPJC 81, 717 (2021)

S. Shi et al., AP 394, 50 (2018)
Y. Jiang et al., CPC 42, 011001 (2018)

Varying the signal using different collision systems: Xe–Xe vs Pb–Pb collisions

ALICE, PLB 856, 138862 (2024)

CME in Xe–Xe collisions

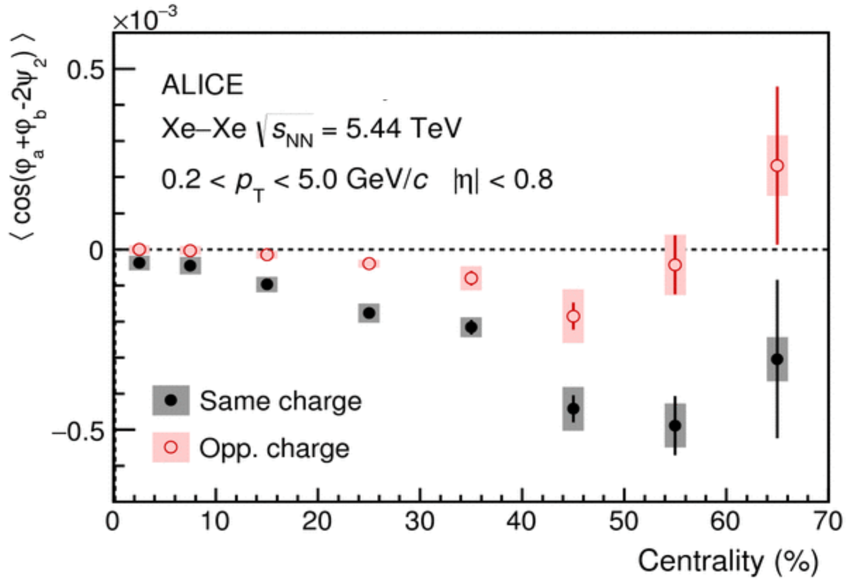

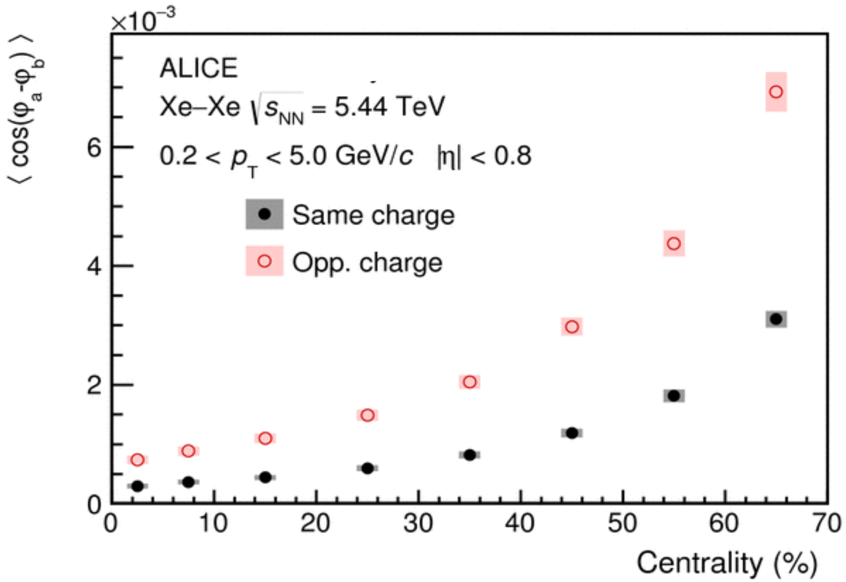

- γ_{ab}: consistent with charge separation
- δ_{ab}: background dominates

Model comparisons

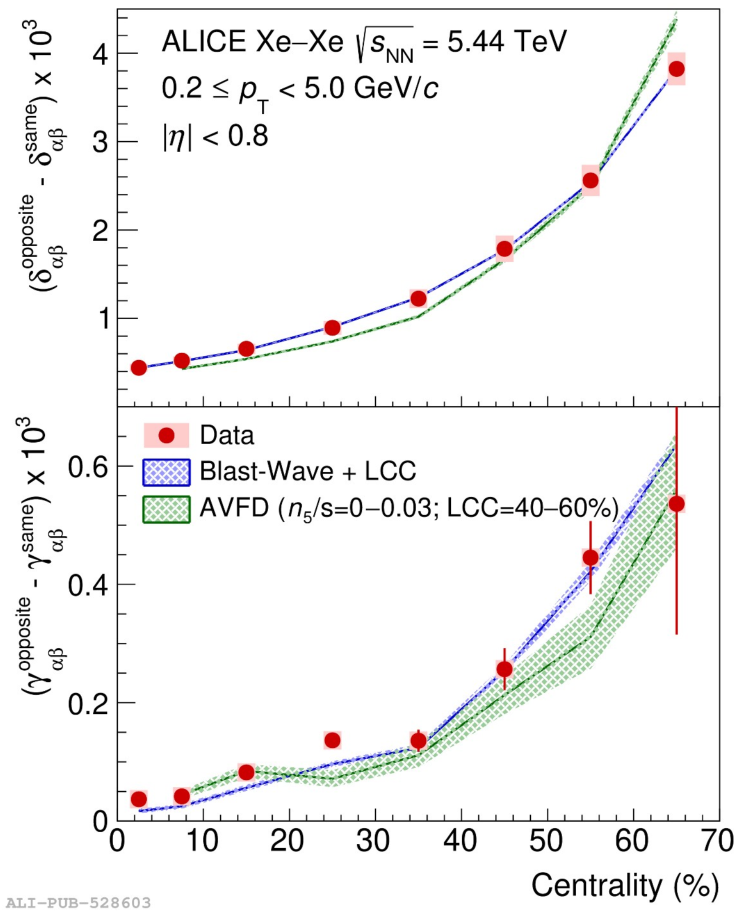

- Blast-Wave + Local Charge Conservation (LCC)
  - Tune the parameters in each centrality class to reproduce v_2 and p_T spectra of π, K, p
  - Tune the number of sources emitting balancing pairs
  - Describes fairly well the measured data points
    - Background dominates measurements
    - Not observed in Pb-Pb collisions

- Anomalous Viscous Fluid Dynamics (AVFD)
  - EbyE IC + E/M fields (field lifetime as input)
  - Tune the parameters in each centrality class to reproduce v_2 and multiplicity P. Christakoglou et al., EPJC 81, 717 (2021)
  - Good agreement with data points
    - Signal consistent with zero

S. Shi et al., AP 394, 50 (2018)
Y. Jiang et al., CPC 42, 011001 (2018)

CME in Xe–Xe and Pb–Pb collisions

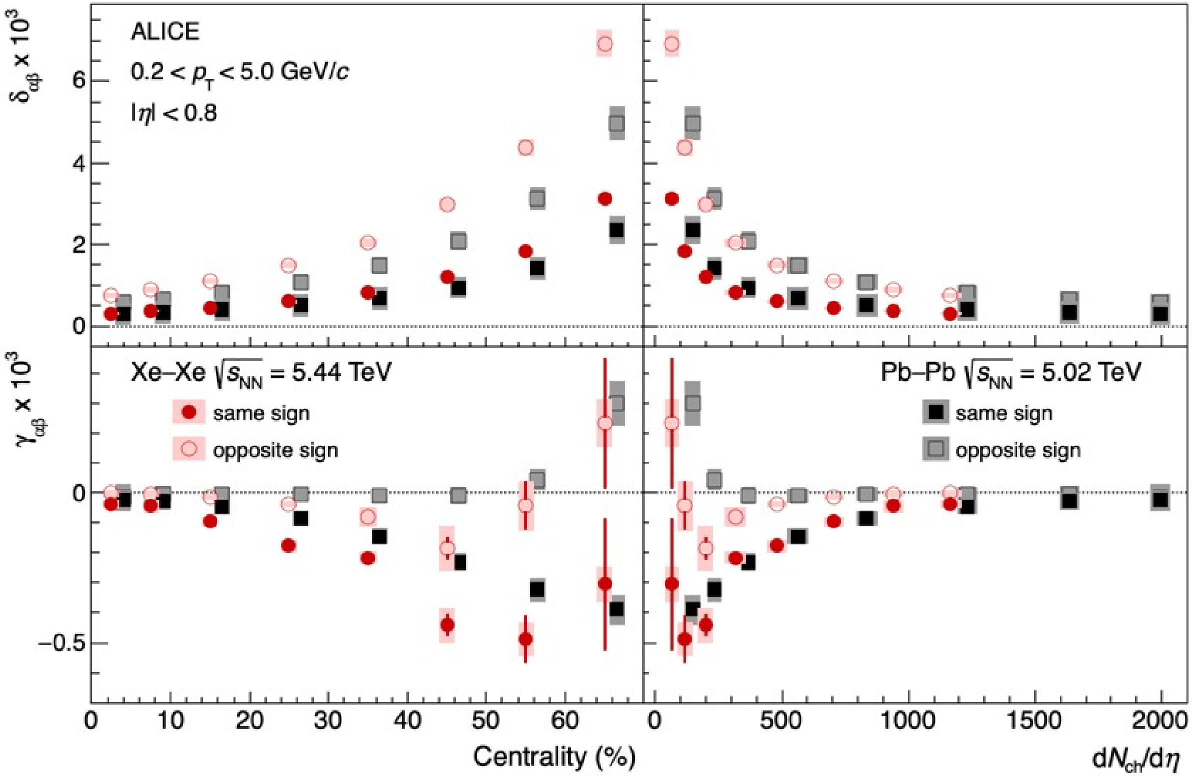

ALICE, JHEP 09, 160 (2020)

ALICE, PRL 116, 222302 (2016)
ALICE, PLB 790, 35 (2019)

- Strong dependence on the charge
- Qualitatively similar centrality dependence
  - Larger magnitude in Xe–Xe than in Pb–Pb collisions
    - Dilution effects arising from different number of particles (CME ~ 1/M)
- Similar values in Xe–Xe and Pb–Pb collisions within uncertainties (vs $dN_{ch}/d\eta$)

CME fraction in Xe–Xe and Pb–Pb collisions

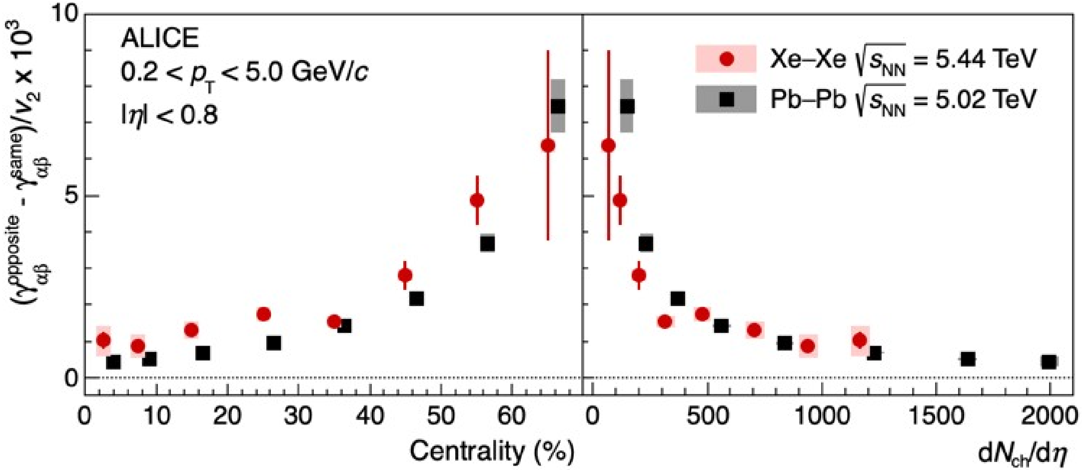

- γ_{ab} (opp-same) can be used to study CME
  - Similar values in Xe–Xe and Pb–Pb collisions (vs $dN_{ch}/d\eta$) → large background contribution

CME fraction in Xe–Xe and Pb–Pb collisions

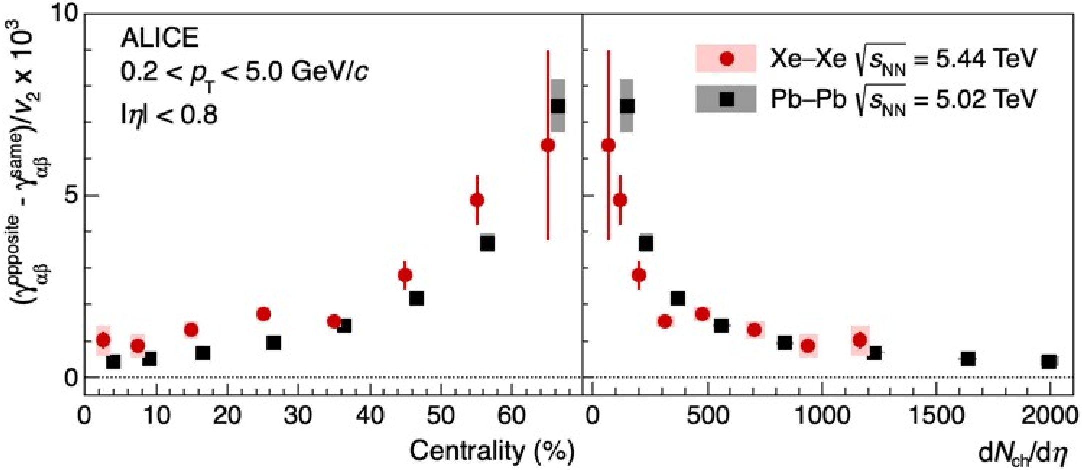

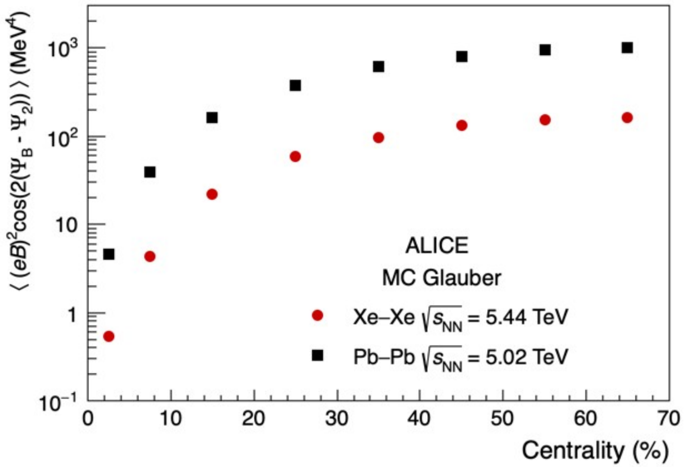

- γ_{ab} (opp-same) can be used to study CME
  - Similar values in Xe–Xe and Pb–Pb collisions (vs $dN_{ch}/d\eta$) → large background contribution

- CME fraction extracted using a two-component approach
  - Assumption: both signal and background scale with $dN_{ch}/d\eta$
    - $dN_{ch}/d\eta$ used to compensate for dilution
  - <$|B|^2\cos(2(\Psi_B-\Psi_2))$> from MC simulations

$$(dN_{ch}/d\eta)^{Xe}\Delta\gamma_{ab}^{Xe} = sB^{Xe} + bv_2^{Xe}$$
$$(dN_{ch}/d\eta)^{Pb}\Delta\gamma_{ab}^{Pb} = sB^{Pb} + bv_2^{Pb}$$

$$f_{CME} = \frac{sB}{sB + bv_2}$$

CME fraction in Xe–Xe and Pb–Pb collisions

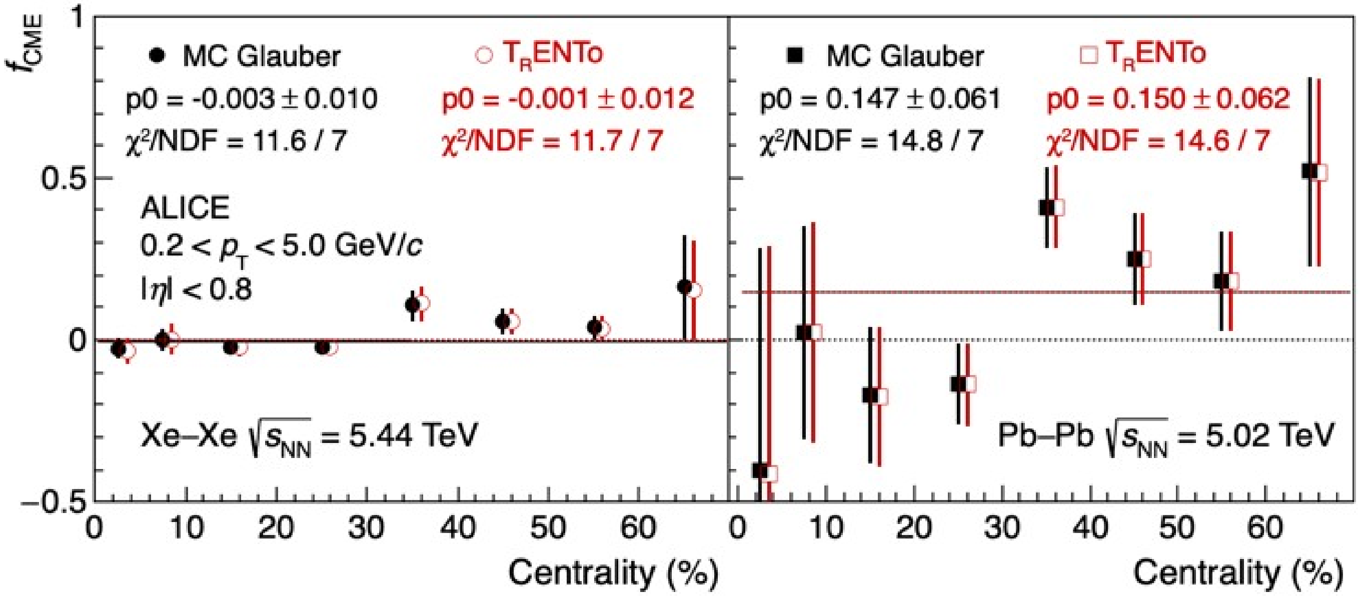

- Consistent with 0 for 0–30% and then becomes positive
- Combining the points from 0–70%
  - f_{CME}^{Xe} = -0.003 ± 0.010 → 2% at 95% C.L.
  - f_{CME}^{Pb} = 0.147 ± 0.061 → 25% at 95% C.L.

$$f_{CME} = \frac{sB}{sB + bv_2}$$

Particle identification

Particle identification (PID) in ALICE

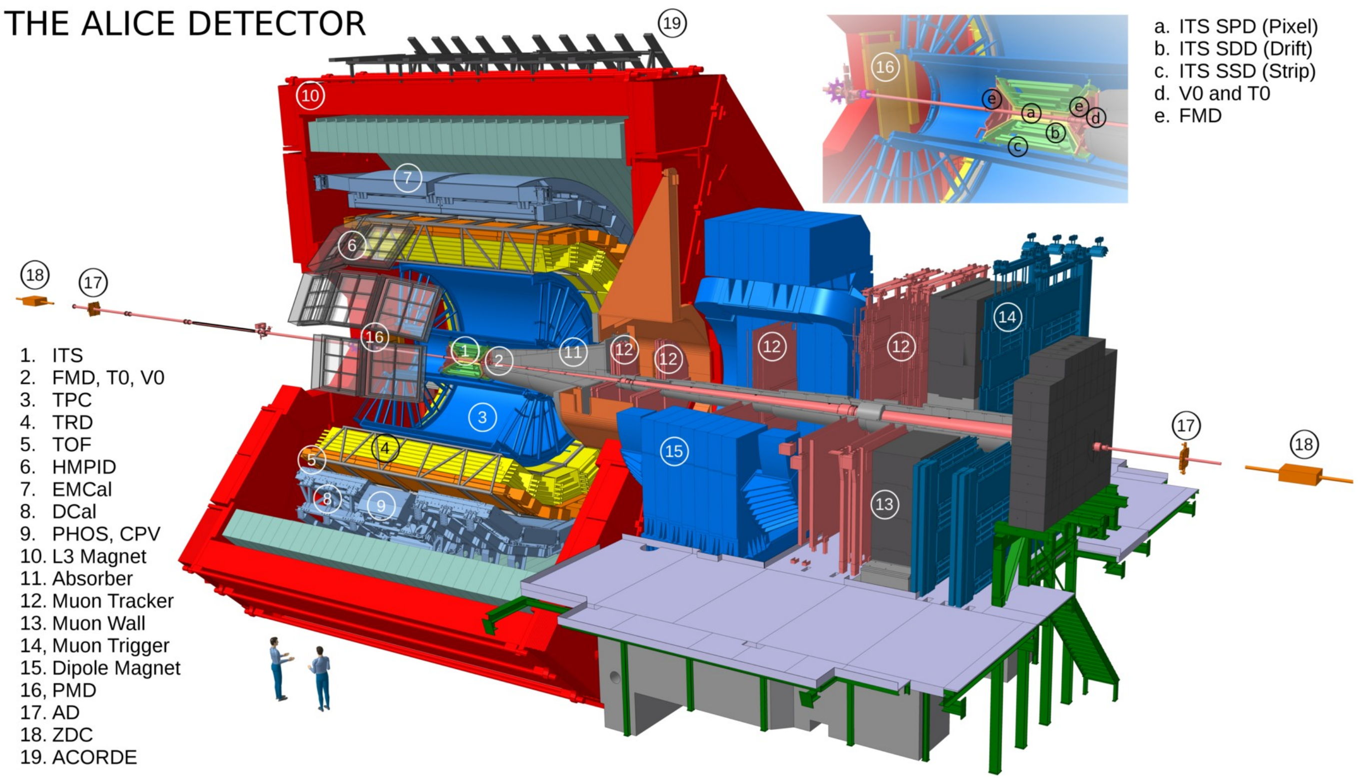

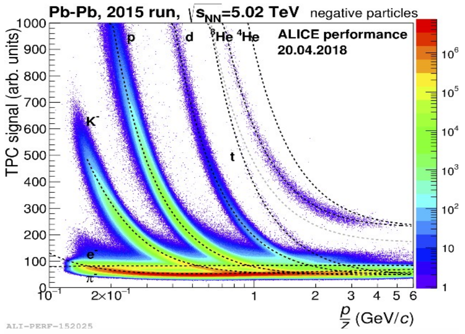

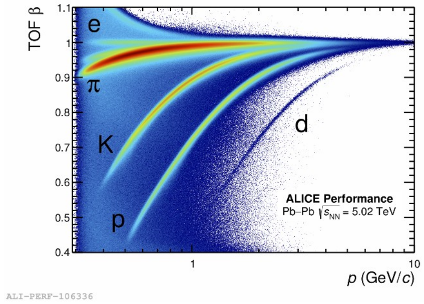

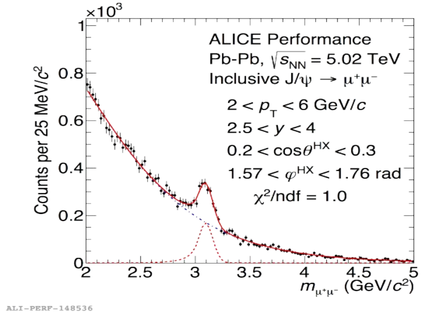

- $\pi^{\pm}$, $K^{\pm}$, p identified using TPC and TOF
- Topological reconstruction for K^0_S, Λ, J/Ψ and D-mesons

CME for h-h, K-K, p-p

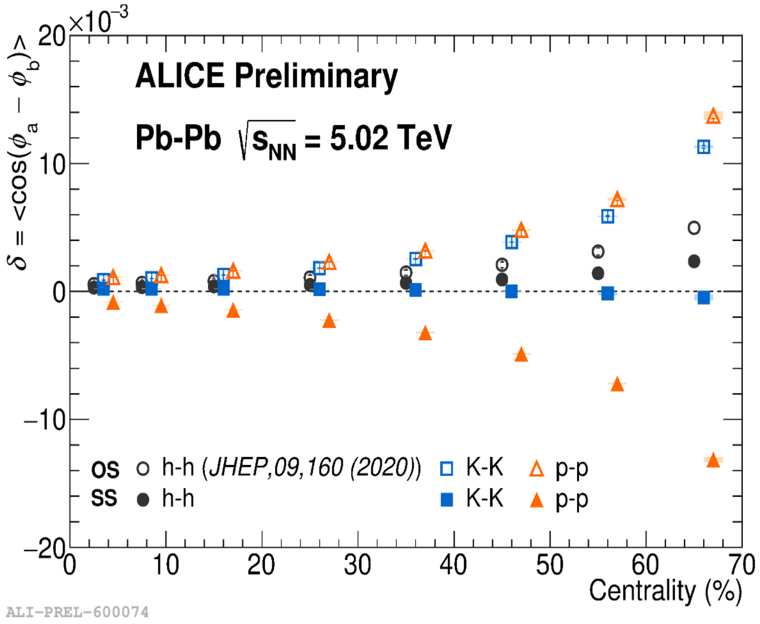

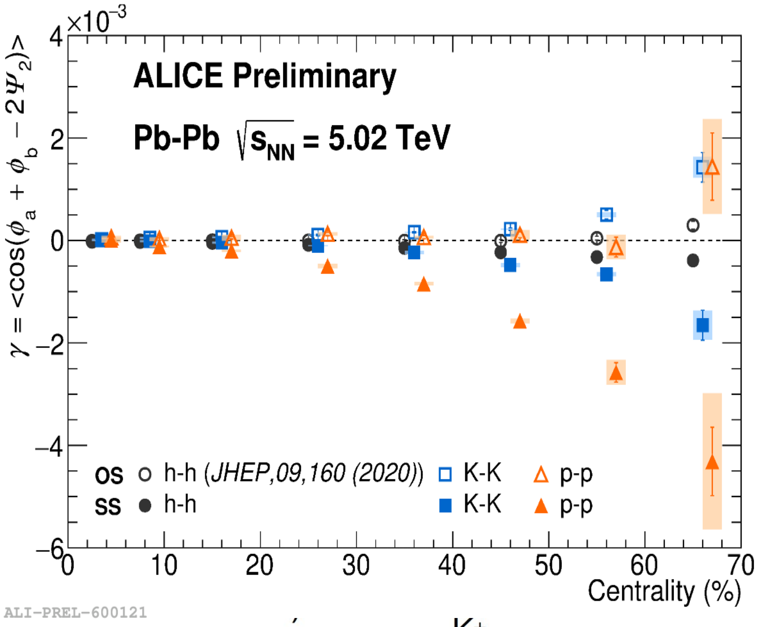

- δ_{ab} and γ_{ab}: strong particle-type dependence (p > K > h)
  - LCC for K-K

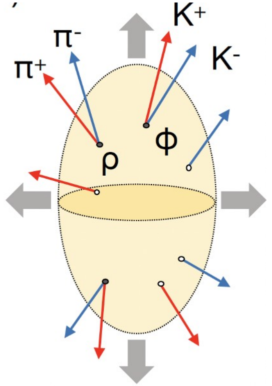

CME for h-h, K-K, p-p

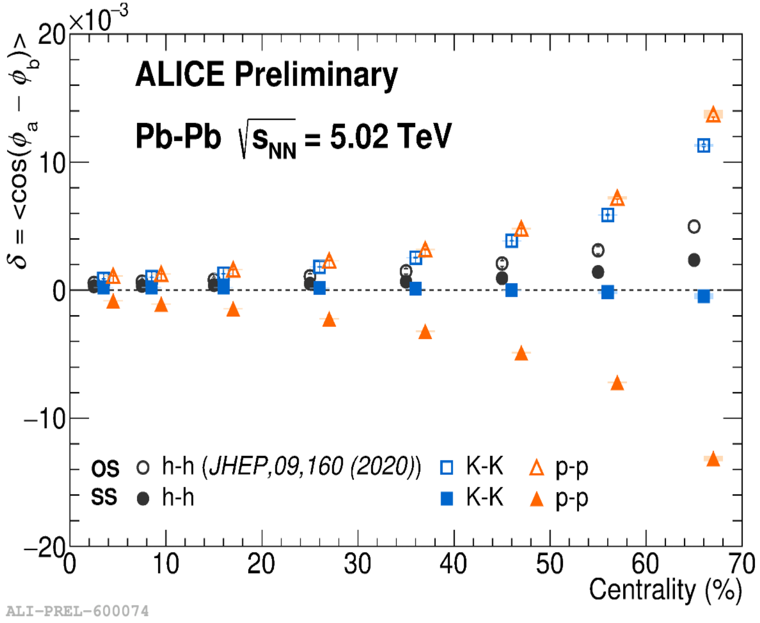

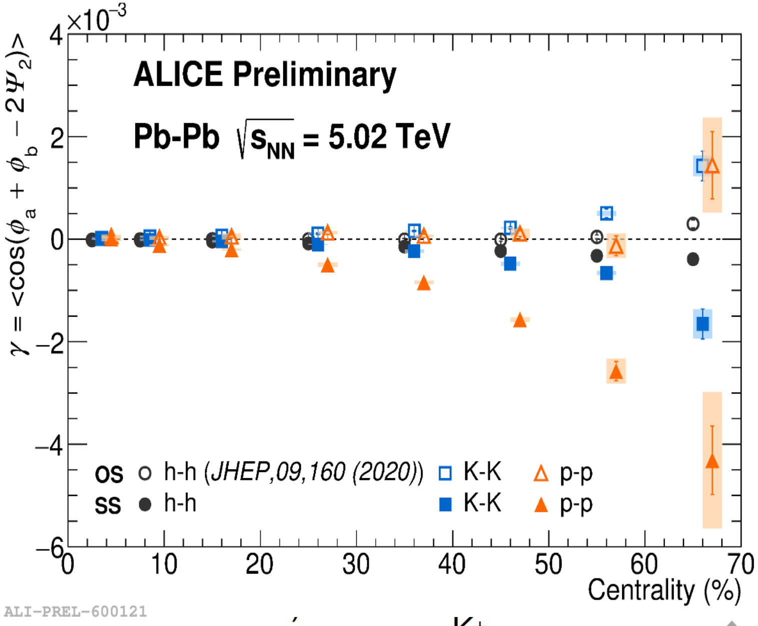

- δ_{ab} and γ_{ab}: strong particle-type dependence (p > K > h)
  - LCC for K-K
  - Coalescence induced local baryon conservation for p-p

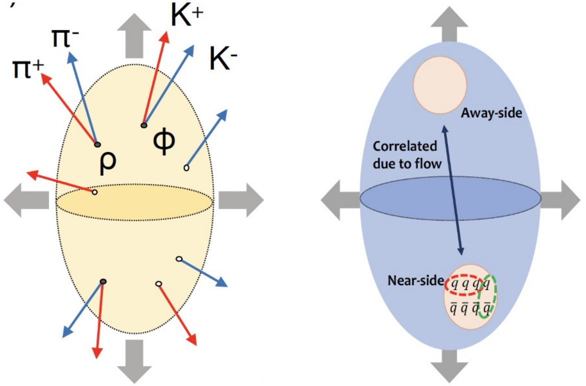

Summary

- Anomalous chiral searches performed in different collision systems
  - Background dominates the measurements
  - Different approaches used to separate the signal from the background

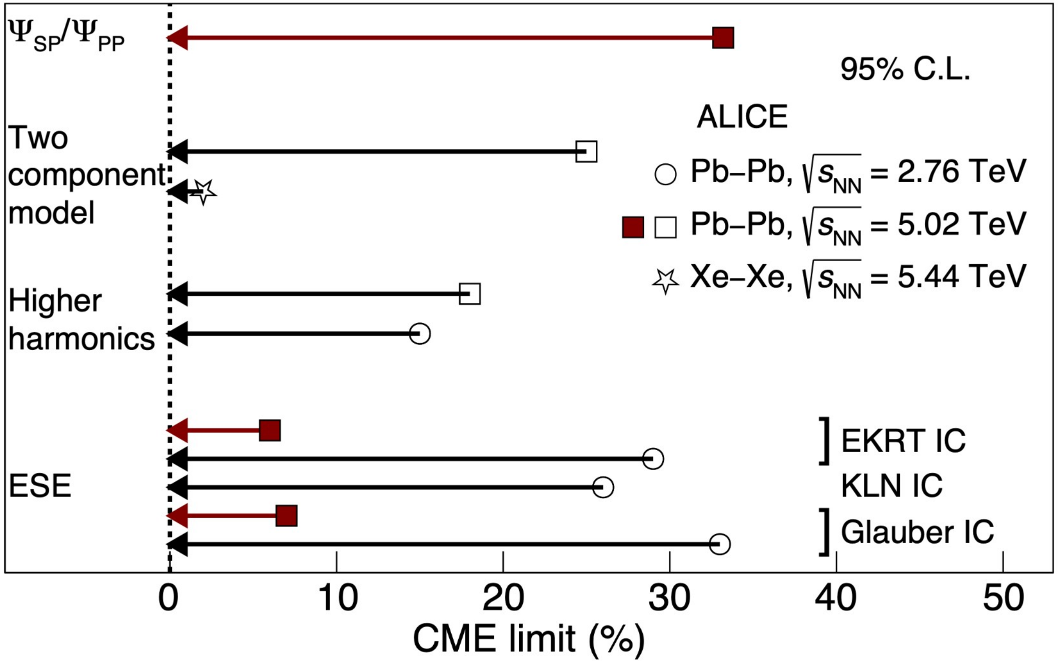

Backup

3-particle correlator: differential results in Xe–Xe and Pb–Pb collisions

ALICE, PLB 856, 138862 (2024)

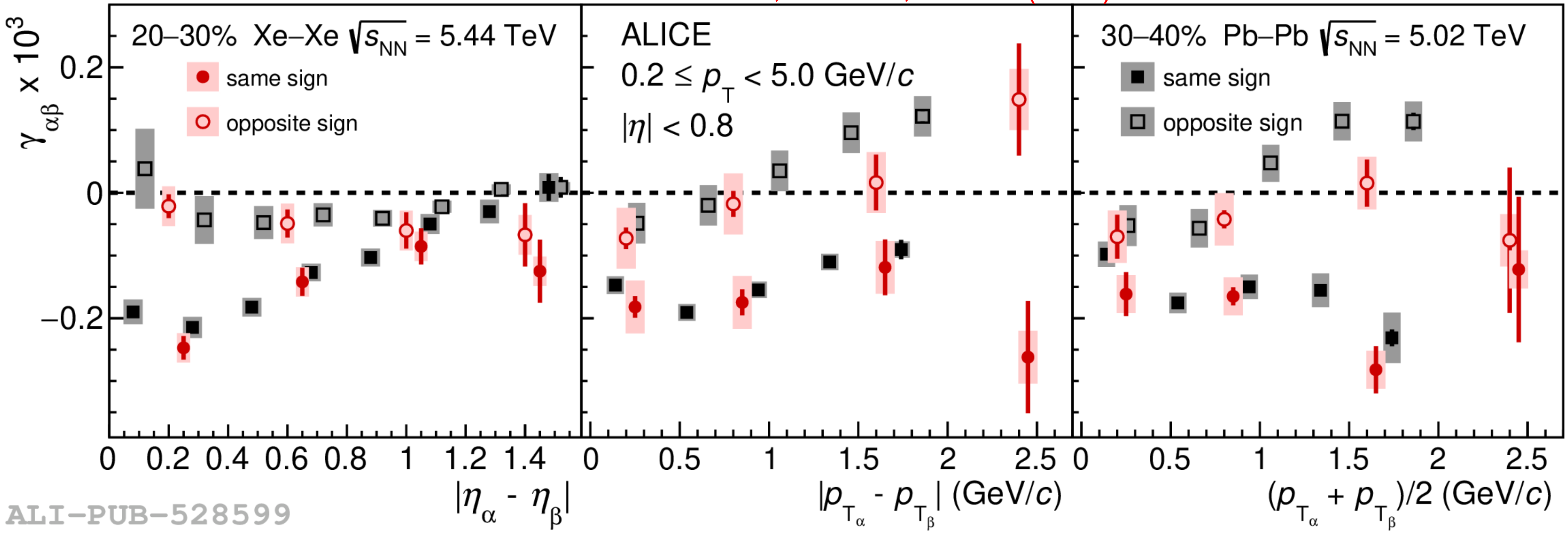

CME for h-h, K-K, p-p, p-Λ

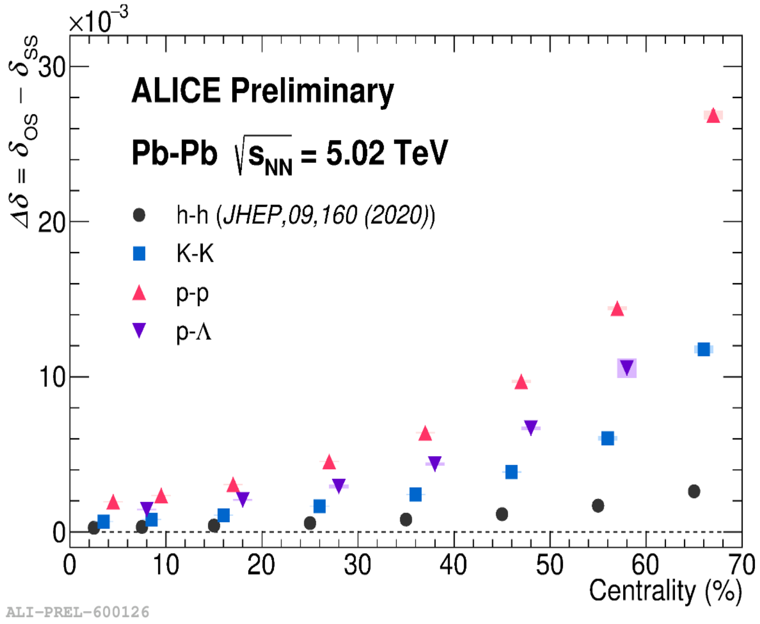

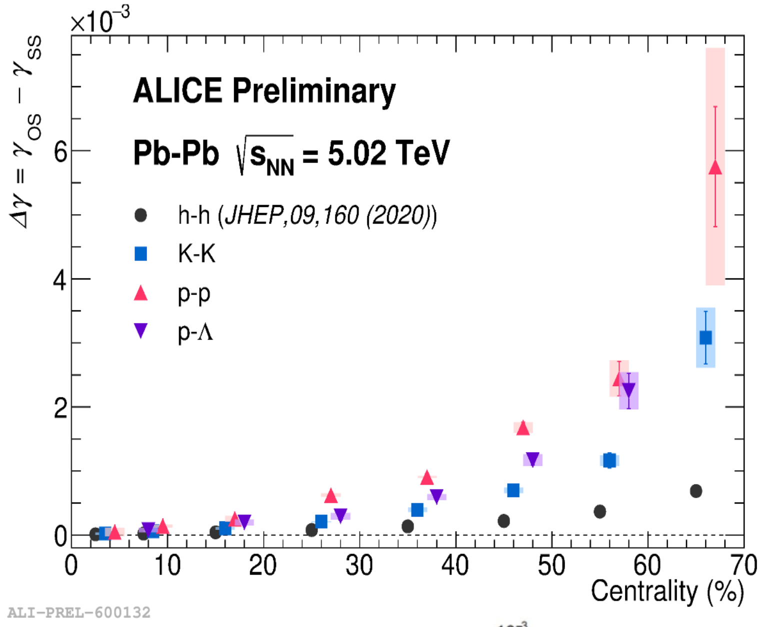

- $\Delta\delta_{ab}$ and $\Delta\gamma_{ab}$: strong particle-type dependence (p-p > p-Λ > K-K > h-h)
  - LCC for K-K
  - Coalescence induced local baryon conservation for p-p

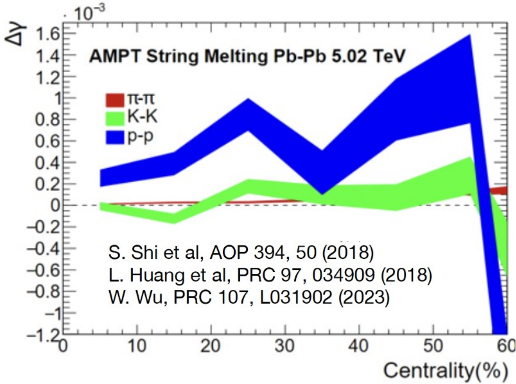

v_2 and $dN_{ch}/d\eta$ in Xe–Xe and Pb–Pb collisions

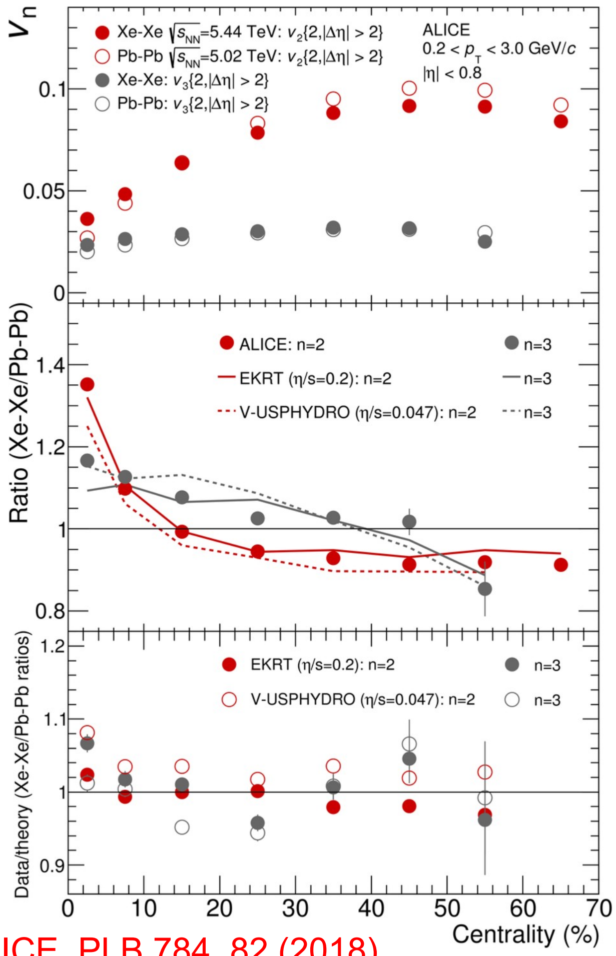

ALICE, PLB 784, 82 (2018)

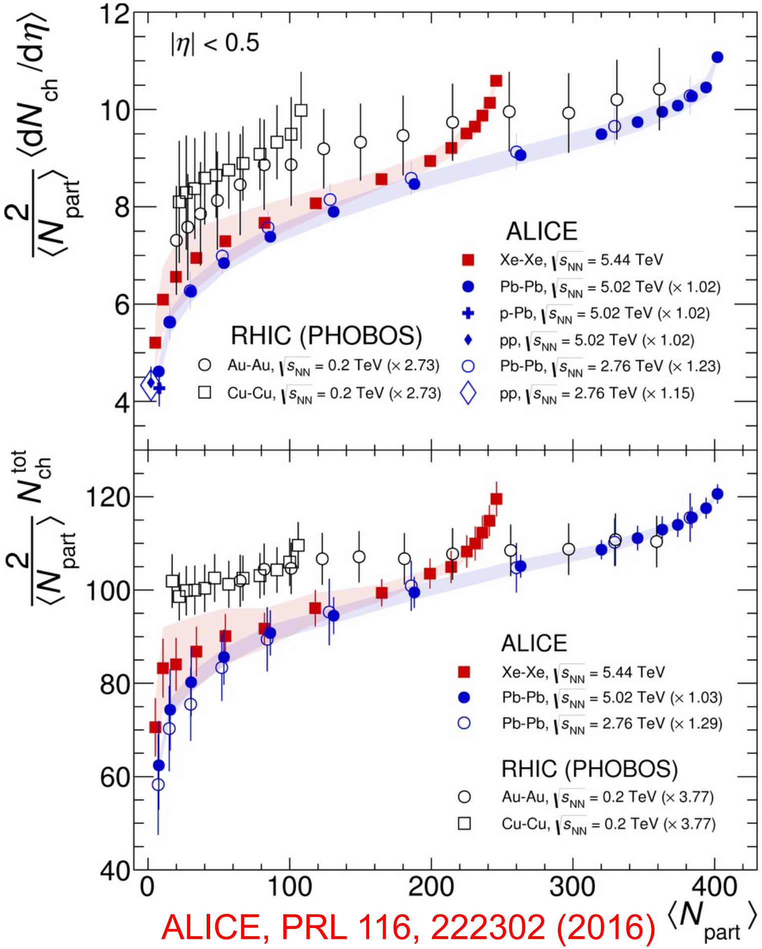

ALICE, PRL 116, 222302 (2016)
ALICE, PLB 790, 35 (2019)

Global polarization of Λ hyperons

ALICE, PRC 101, 044611 (2020); ALICE, PRC 105, 029902 (2022)

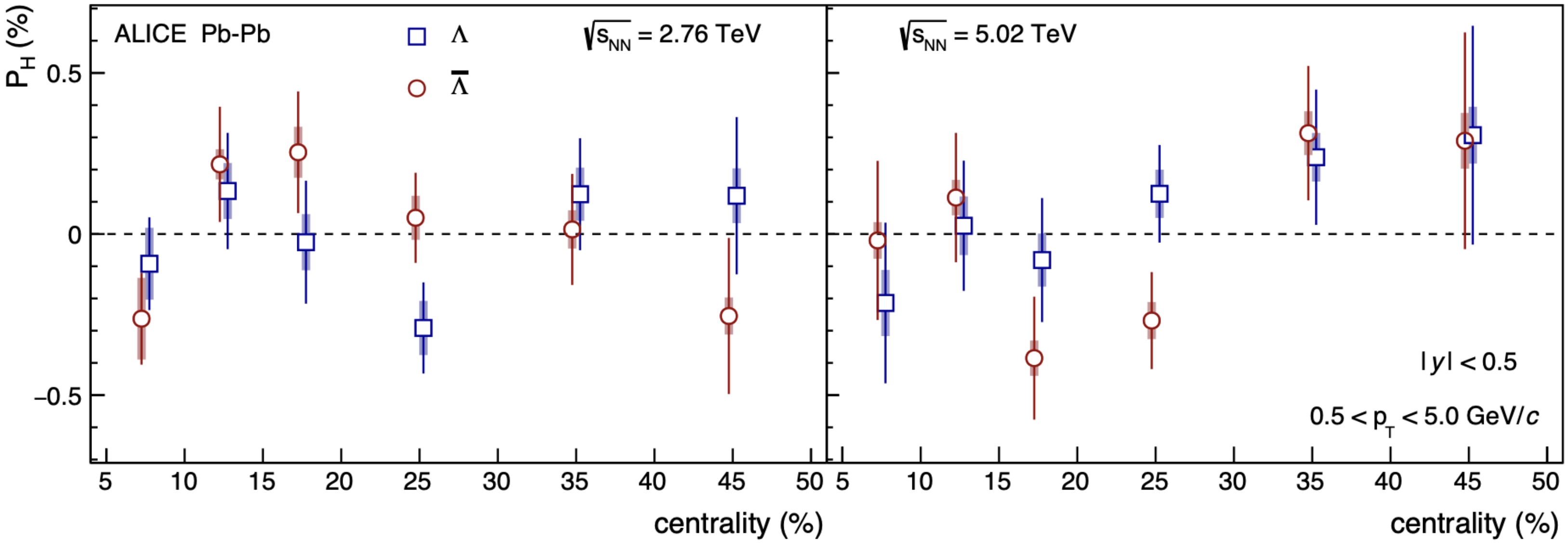

$\sqrt{s_{NN}}$	centrality	P_Λ (%)	$P_{\bar{\Lambda}}$ (%)
2.76 TeV	5–15%	-0.01 ± 0.12 (stat.) ± 0.04 (syst.)	-0.08 ± 0.12 (stat.) ± 0.07 (syst.)
	15–50%	-0.07 ± 0.09 (stat.) ± 0.04 (syst.)	0.05 ± 0.09 (stat.) ± 0.03 (syst.)
5.02 TeV	5–15%	-0.07 ± 0.16 (stat.) ± 0.07 (syst.)	0.06 ± 0.16 (stat.) ± 0.03 (syst.)
	15–50%	0.12 ± 0.10 (stat.) ± 0.04 (syst.)	-0.13 ± 0.11 (stat.) ± 0.03 (syst.)
average	15–50%	$\langle P_H \rangle$ (%) $\approx -0.01 \pm 0.05$ (stat.) ± 0.03 (syst.)	

- P_H consistent with zero

$$P_{\Lambda,\bar{\Lambda}} = \pm \frac{8}{\pi \alpha_{\Lambda,\bar{\Lambda}}} \times \frac{\langle \sin(\phi_p^* - \Psi_{RP}) \rangle}{R_{RP}}$$

Global polarization of Λ hyperons: magnetic field estimation

ALICE, PRC 101, 044611 (2020); ALICE, PRC 105, 029902 (2022)

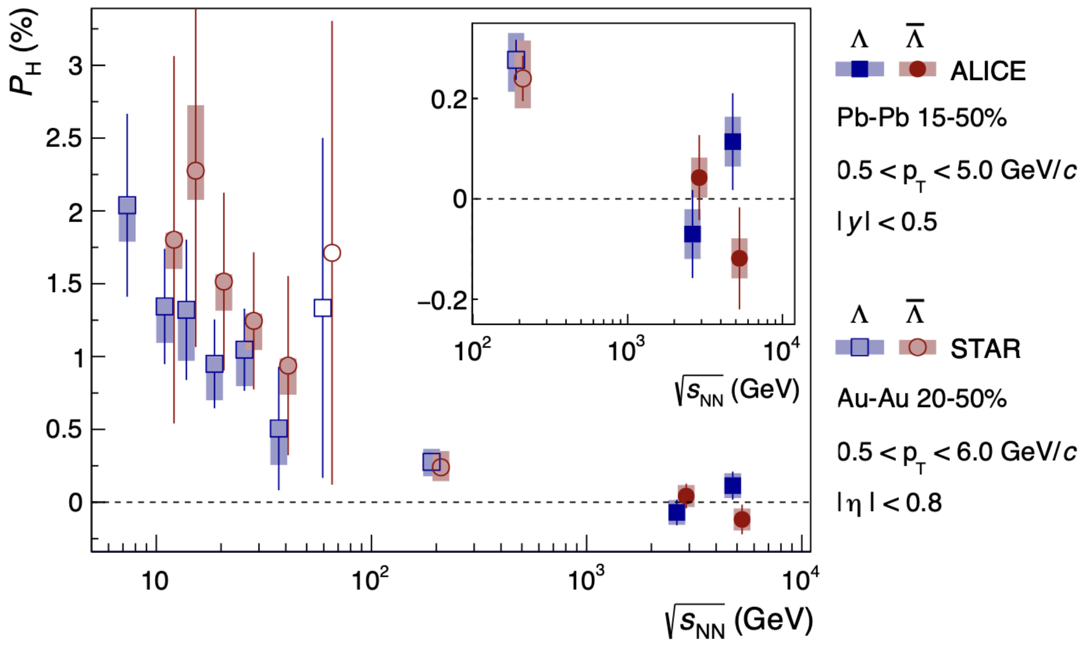

Global polarization of Λ hyperons: magnetic field estimation

ALICE, PRC 101, 044611 (2020); ALICE, PRC 105, 029902 (2022)

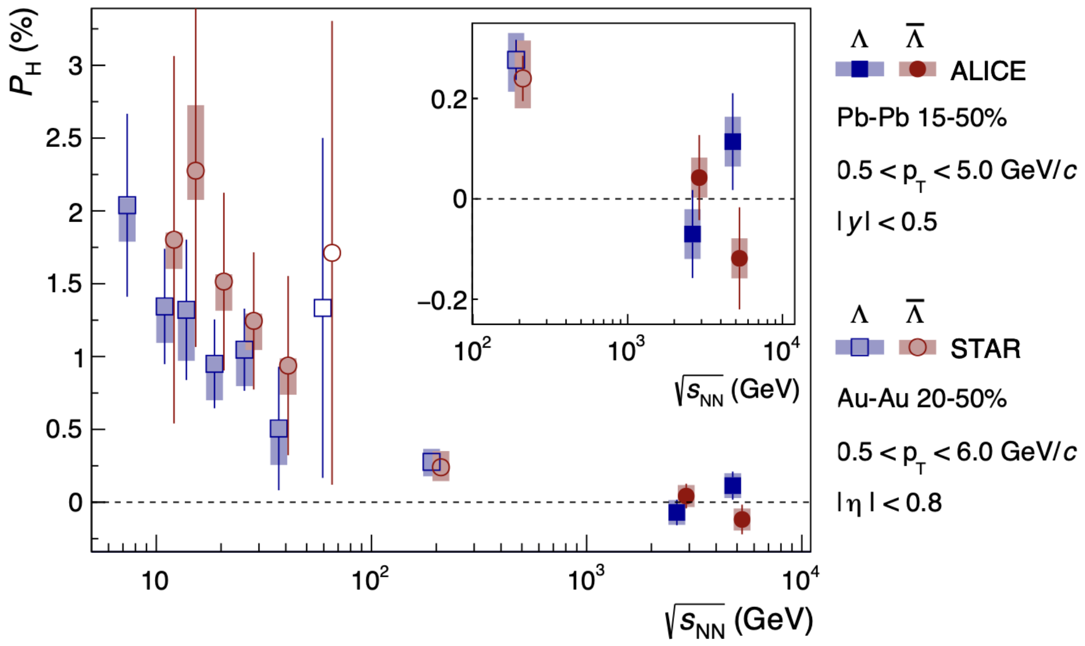

ALICE, EPJC 84, 813 (2024)

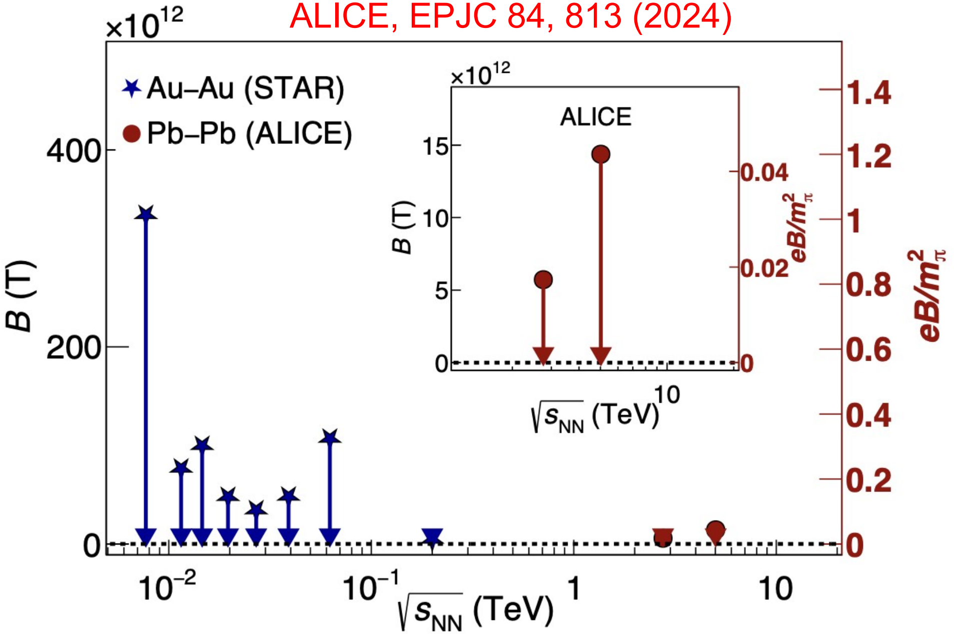

$$P_\Lambda \approx 0.5\omega/T + |\mu_\Lambda|B/T$$

$$P_{\bar{\Lambda}} \approx 0.5\omega/T - |\mu_\Lambda|B/T$$

Magnetic field evidence

- Search for magnetic-induced charge currents using charge-dependent v_1
  - Faraday and Hall effects (competing effects)

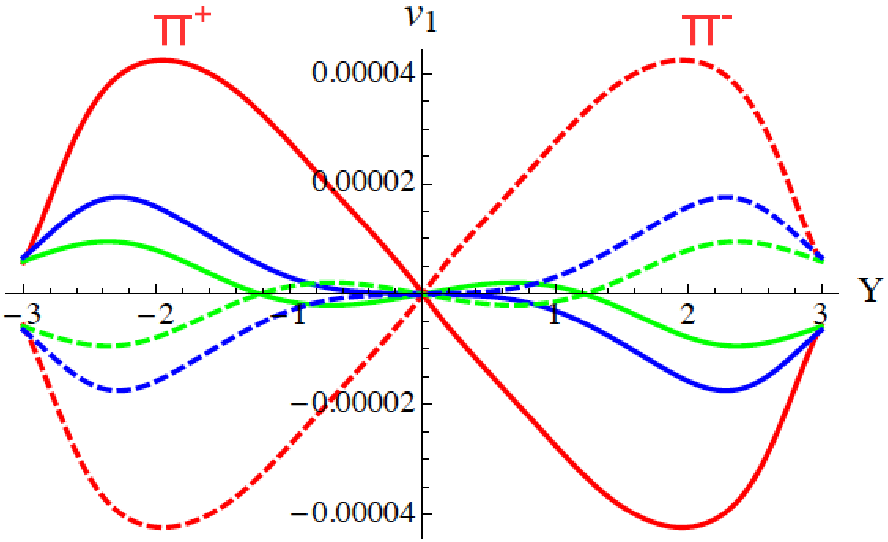

Pb-Pb $\sqrt{s_{NN}}$=2.76 TeV, p_T = 0.25, 0.5, 1 GeV/c

U. Gursoy et al., PRC 89, 054905 (2014)

- Rapidity slope of $\Delta v_1 = v_1^+ - v_1^-$ expected to vary with p_T

$$v_1^{t,p} = \frac{\langle \mathbf{u}\mathbf{Q}^{t,p}\rangle}{\sqrt{\left|\langle \mathbf{Q}^t\mathbf{Q}^p\rangle\right|}} = \frac{\langle \mathrm{u_x}Q_x^{t,p} + \mathrm{u_y}Q_y^{t,p}\rangle}{\sqrt{\left|\langle Q_x^tQ_x^p + Q_y^tQ_y^p\rangle\right|}}$$

$$\mathbf{Q}^{t,p} \equiv (Q_x^{t,p}, Q_y^{t,p}) = \sum_{i=1}^{4}\mathbf{n}_iE_i^{t,p} \Big/ \sum_{i=1}^{4}E_i^{t,p}$$

$$\mathbf{u} = (\cos\varphi, \sin\varphi)$$

Magnetic field evidence

- Search for magnetic-induced charge currents using charge-dependent v_1
  - Faraday and Hall effects (competing effects)

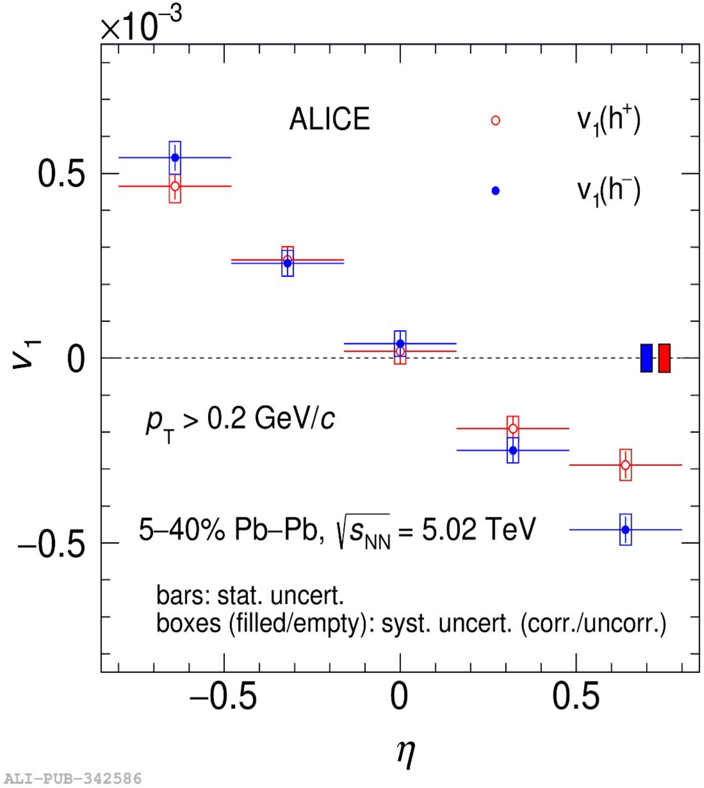

- Measurements performed for v_1^{odd} of charged particles

Magnetic field evidence

- Search for magnetic-induced charge currents using charge-dependent v_1
  - Faraday and Hall effects (competing effects)

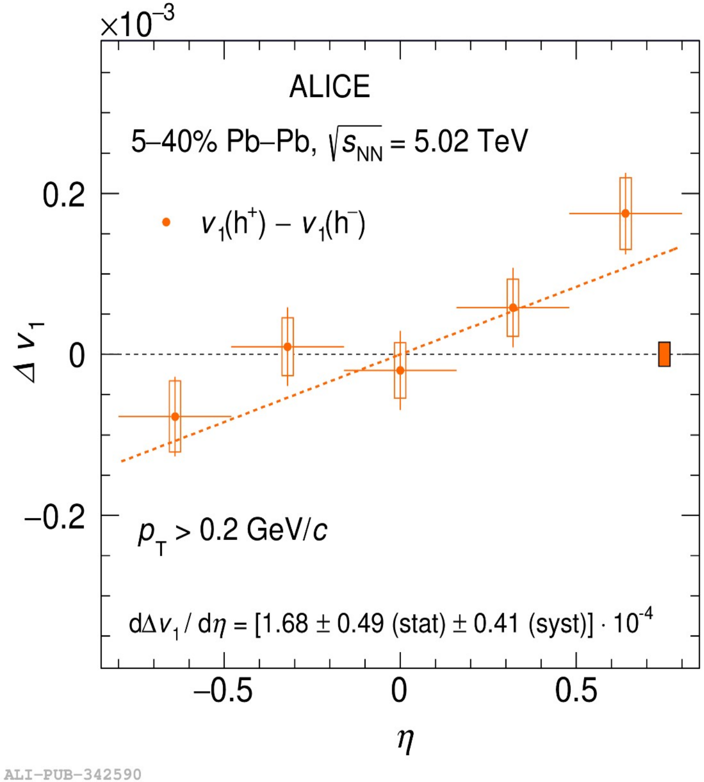

- Measurements performed for v_1^{odd} of charged particles
  - Non-zero slope measured with a significance of 2.6σ

Magnetic field evidence

- Search for magnetic-induced charge currents using charge-dependent v_1
  - Faraday and Hall effects (competing effects)

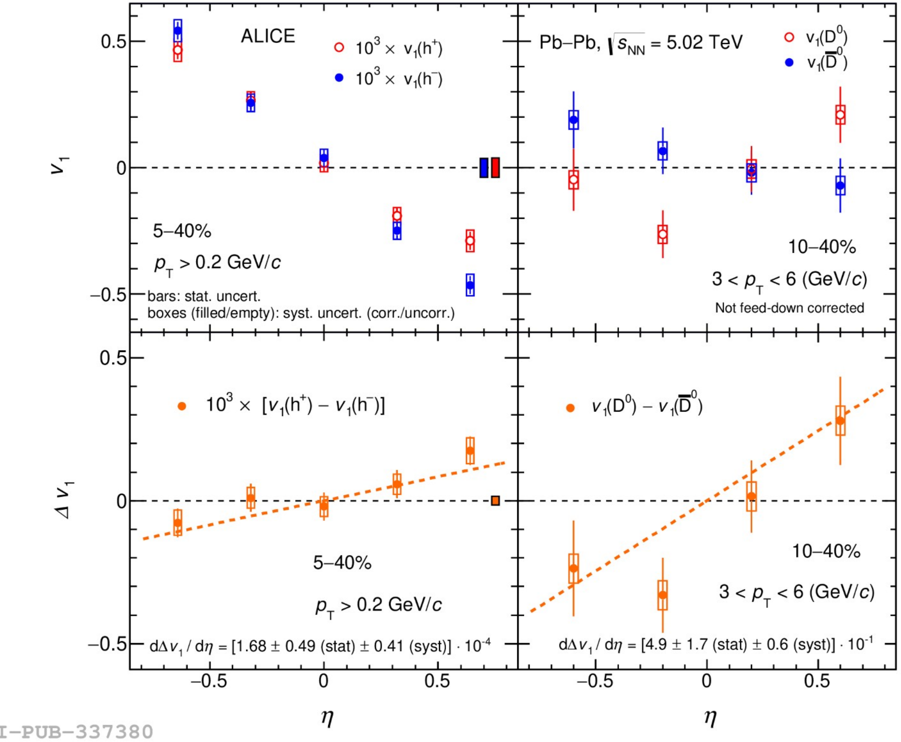

- Measurements performed for v_1^{odd} of charged particles
  - Non-zero slope measured with a significance of 2.6σ
- and for v_1^{odd} of D^0 mesons
  - Non-zero slope measured with a significance of 2.7σ
    - 3 orders of magnitude larger than the one of the charged hadrons

Magnetic field evidence

- Search for magnetic-induced charge currents using charge-dependent v_1
  - Faraday and Hall effects (competing effects)

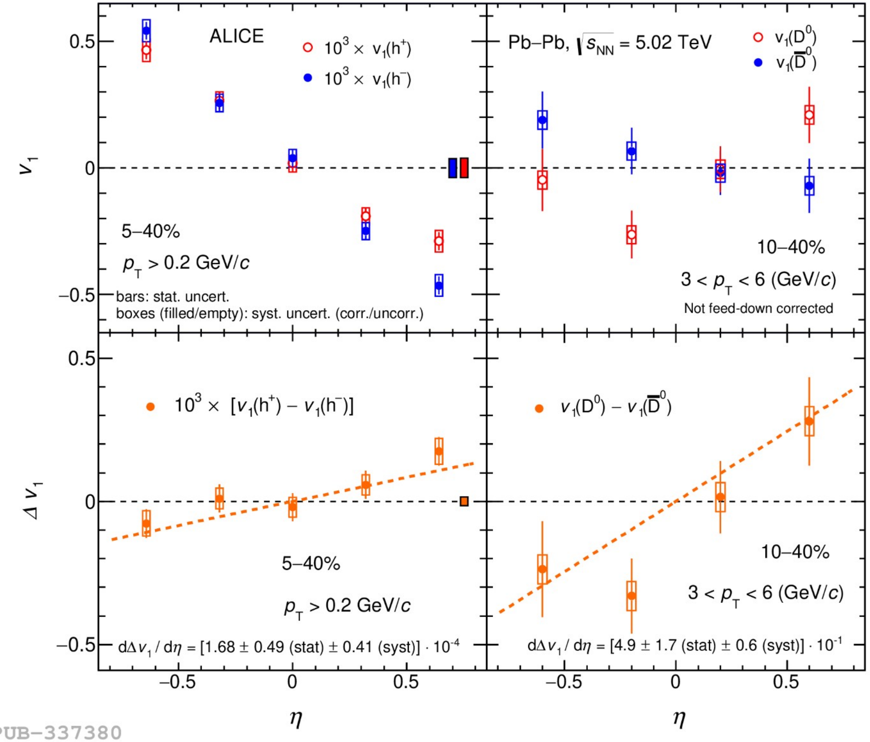

- Measurements performed for v_1^{odd} of charged particles
  - Non-zero slope measured with a significance of 2.6σ
- and for v_1^{odd} of D^0 mesons
  - Non-zero slope measured with a significance of 2.7σ
    - 3 orders of magnitude larger than the one of the charged hadrons
- 1-2 orders of magnitude bigger and opposite sign (mostly Hall effect?)
- Important baseline for searches of the CME

ALI-PUB-337380